TABLE 1. Absolute Copy Numbers of Specific Cell Marker mRNA in Cultivated Cells

	Copy Numbers of mRNA/μg of Total RNA	
	NC Cells (n=6)	Lymph Node Cells (n=6)
CD3	37 600±6300	1 490 000±215 000
Collagen type III	149 000 000±10 500 000	170 000±15 000
Calponin	23 400 000±2 110 000	ND
CD11b	11 800 000±977 000	19 000±4200
von Willebrand factor	194 000±31 000	262 000±56 000
α-Cardiac myosin	ND	ND

Results are expressed as mean±SEM.

muscle cells, and endothelial cells) by anti-PE micro beads (Miltenyi Biotec) and an MACS magnetic cell sorting system (Miltenyi Biotech) using appropriate monoclonal antibodies, namely PE-conjugated TCRα/β (R73) and CD11bc (OX-42) (Pharmingen).[26] The fractions of cardiomyocytes, αβT cells, $CD11b^+$ cells, and NCNI cells were confirmed by analysis of specific marker gene expression—α-cardiac myosin, CD3, CD11b, collagen type III, calponin, and von Willebrand factor—and even if the level of contamination was the highest, it was <10% (data not shown). Total RNA was isolated from each purified cell fraction (cardiomyocytes, n=5; αβT cells, n=5; $CD11b^+$ cells, n=5; NCNI cells, n=6). The absolute copy numbers of IL-1 family mRNA were measured by quantitative real-time RT-PCR.

Cell Culture With Serum Containing IL-1RA-Ig

NC Cells

On day 18, NC cells were isolated from the hearts of EAM rats via collagenase preparation and were cultured for 1 week on 35-mm–well dishes in 3 mL RPMI medium supplemented with 10% FCS. These cultivated NC cells were suggested to contain mainly fibroblasts, smooth muscle cells, and $CD11b^+$ cells, as determined by gene expression analysis (Table 1). After reaching confluence, NC cells were stimulated by addition of 10 ng/mL IL-1α (Pepro Tech) and 100 μL IL-1RA-Ig-Glu-tag–containing serum (30 nmol/L) or the same amount of Ig-Glu tag–containing serum (IL-1RA-Ig+IL-1α group, n=6; SP-Ig+IL-1α group, n=6; no serum and no IL-1α group, n=6). After culture for 24 hours at 37°C, NC cells were collected and total RNA was isolated. The absolute copy numbers of γ-actin, prostaglandin E synthase (PGES), cyclooxygenase-2 (Cox-2), and IL-1β mRNA were measured by quantitative real-time RT-PCR.

Lymphocytes

Lymphocytes isolated from popliteal lymph nodes of EAM rat were prepared in 3 mL RPMI medium supplemented with 10% FCS in 35-mm–well dishes. These cells were thought to be mainly lymphocytes, as indicated by expression of the CD3 gene (Table 1). Because transfer of concanavalin A (Con-A)–stimulated lymphocytes from EAM popliteal lymph nodes could induce EAM[27] and Con-A–stimulated lymphocytes can express the IL-1RI gene (data not shown), we stimulated these cells with 10 μg/mL Con-A (Sigma) and 10 ng/mL IL-1α at 6×10^6 cells per dish. One hundred microliters of IL-1RA-Ig-Glu-tag–containing serum (30 nmol/L) or the same amount of Ig-Glu-tag–containing serum was added (IL-1RA-Ig+Con-A+IL-1α, n=6; SP-Ig+Con-A+IL-1α, n=6; no serum, no Con-A, and no IL-1α, n=6). After culture for 24 hours at 37°C, these cells were collected and total RNA was isolated. The absolute copy numbers of γ-actin, IL-2, and IFN-γ mRNA were measured by quantitative real-time RT-PCR.

Quantitative Real-Time RT-PCR Analysis

Total RNA was extracted by use of Trizol (Invitrogen). cDNA was synthesized from 2 to 5 μg total RNA with random primers and murine Moloney leukemia virus RT. To create the plasmids used for the standard, the cDNAs for ANP, specific cell markers, IL-1 family proteins, and immunologic molecules were amplified from an EAM heart–derived cDNA library with the primers indicated in Table 2. PCR-amplified cDNA inserts were directly inserted into the pGEM-T easy vector, and the recombinant plasmids were isolated, after transformation into *E coli* JM109 competent cells, with the MagExtractor plasmid kit (Toyobo). Diluted plasmid and cDNA were amplified via real-time RT-PCR with a Lightcycler, together

TABLE 2. List of Primers for Quantitative RT-PCR

	Sense Primer	Antisense Primer
ANP	5′-atggatttcaagaacctgctagac-3′	5′-gctccaatcctgtcaatcctac-3′
α-Cardiac myosin	5′-acaaggttaaaaacctgacagagg-3′	5′-tactgttctgctgactgatgtcaa-3′
CD3	5′-gatcccaaactctgctatatgcta-3′	5′-ctttcatgccaatctcactgtag-3′
CD11b	5′-gggatccgtaaagtagtgagaa-3′	5′-aaaggagctggtacttcctgtct-3′
Collagen type III	5′-cgcaattgcagagacctgaa-3′	5′-acagtcatgggactggcatttat-3′
von Willebrand factor	5′-agaggctacacatctctcagaagc-3′	5′-gaccttcttcttcttgaaaccttg-3′
Calponin	5′-aacataggaaatttcatcaaagcc-3′	5′-gtagactgatagttgcctgatcca-3′
IL-1α	5′-aagttcctgacttgtttgaagacc-3′	5′-gtcatcttcagtaaagggctgatt-3′
IL-1β	5′-gctagtgtgtgatgttcccattag-3′	5′-cttttccatcttcttctttgggta-3′
IL-1RI	5′-ataaactgatggtgatgaatgtgg-3′	5′-tgagagtgaactttcttttggctg-3′
IL-1RII	5′-gttatgacatttacctacgagggc-3′	5′-ctttgtgactggatcaaaaatcag-3′
IL-1Racp	5′-ctggacttaccctgatctggtacg-3′	5′-acacgtgatattgtgaataccctg-3′
sIL-1RA	5′-tctctctccttctcatccttctgt-3′	5′-atcagtgatgttaacctcctccag-3′
Total IL-1RA	5′-agaagaaaagatagacatggtgcc-3′	5′-actttgtgactgtacagggctctt-3′
IL-2	5′-ctgagagggatcgataattacaaga-3′	5′-attggcactcaaatttgttttcag-3′
IFN-γ	5′-atctggaggaactggcaaaaggacg-3′	5′-ccttaggctagattctggtgacagc-3′
PGES	5′-gtgatggagaacagccaggt-3′	5′-gaggaccacgaggaaatgtatc-3′
Cox-2	5′-tgtgatattctcaaacaggagcat-3′	5′-aaggaggatggagttgttgtagag-3′
γ-Actin	5′-agccttccttcctgggcatggagt-3′	5′-tggaggggcctgactcgtcatact-3′

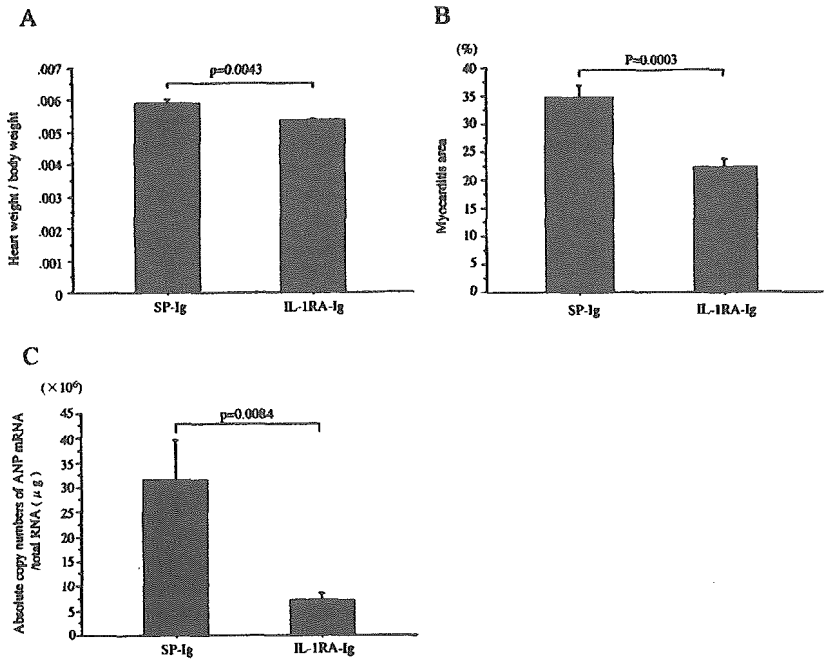

Figure 1. A, Ratio of heart weight to body weight. B, Myocarditis area in EAM heart. Area was calculated by color image analyzer using specimens stained with Azan-Mallory. C, Absolute copy number of ANP mRNA in EAM hearts. Error bars represent SEM. Statistical assessment was performed by unpaired Student *t* test. SP-Ig indicates rats that were injected with pCAGGS-rat SP-Ig-Glu-tag; IL-1RA-Ig, rats injected with pCAGGS-mouse IL-1RA-Ig-Glu-tag.

with the same primer pair used for making the plasmid and a LightCycler-FastStart DNA Master SYBR Green I kit (Roche). After an initial denaturation step of 10 minutes at 95°C, a 3-step cycling procedure (denaturation at 95°C for 10 seconds, annealing at 62°C for 10 seconds, and extension at 72°C for 13 seconds) was used for 40 cycles. The absolute copy numbers of particular transcripts were calculated by LightCycler software using a standard curve approach.[4] cDNA from cultivated cells was then subjected to quantitative RT-PCR analysis, with the level of γ-actin mRNA acting as an internal control.

Statistical Analysis

Statistical assessment was performed by unpaired Student *t* test or 1-way ANOVA and Bonferroni multiple comparison test. The differences were considered significant at $P<0.05$. Ratio of heart weight to body weight, myocarditis area, echocardiography and hemodynamic parameters, data obtained from quantitative RT-PCR, and concentration of IL-1RA-Ig-Glu-tag and Ig-Glu-tag were expressed as mean±SEM.

Results

Effect of In Vivo Treatment With Plasmid DNA Encoding IL-1RA-Ig Gene

The heart to body weight ratios in the IL-1RA-Ig group were significantly lower than those of the SP-Ig group (mean±SEM, 0.53±0.03% versus 0.59±0.05%; $P=0.0043$) (Figure 1A). The inflammatory area in the IL-1RA-Ig group was significantly smaller than that observed in the SP-Ig group (22.3±4.8% versus 34.6±6.8%, $P=0.0003$) (Figure 1B). Expression of ANP mRNA (a heart failure marker) was significantly lower in heart tissues of the IL-1RA-Ig group than those of controls (7.13×10^6±3.62×10^6 versus 31.6×10^6±24.2×10^6 copy/total RNA μg; $P=0.0084$) (Figure 1C).

Echocardiograph and Hemodynamic Parameters

As shown in Table 3, the LV fractional shortening and the absolute value of +dP/dt or −dP/dt in IL-1RA-Ig group were significantly larger than in SP-Ig group. LV end-systolic diameter, LV posterior wall thickness, PE, LV end-diastolic pressure, and central venous pressure were significantly smaller in the IL-1RA-Ig group than in SP-Ig group.

Time Course of IL-1RA-Ig-Glu-Tag Protein Levels

Plasma IL-1RA-Ig-Glu-tag protein levels in the IL-1RA-Ig group were found to increase, peaking at 23.21±8.52 nmol/L (mean±SEM) on day 2, and gradually decrease to 5.56±2.70 nmol/L on day 5, 1.64±0.63 nmol/L on day 8, 0.85±0.45 nmol/L on day 12, and 0.22±0.07 nmol/L on day 17. The plasma Ig-Glu-tag protein levels in the SP-Ig group were seen

TABLE 3. Echocardiographic and Hemodynamic Parameters

	IL-1RA-Ig (n=7)	SP-Ig (n=6)	*P*
LVEDd, mm	5.41±0.05	5.48±0.29	0.81
LVESd, mm	3.01±0.17	3.81±0.24	0.018
IVS, mm	1.84±0.05	1.96±0.12	0.33
LVPW, mm	1.89±0.17	2.24±0.27	0.012
PE, mm	1.71±0.47	3.67±0.49	0.016
LVFS, %	44.4±2.9	30.4±2.4	0.0039
HR, bpm	354.9±14.3	381.5±19.8	0.29
CVP, mm Hg	1.73±0.26	3.93±0.55	0.0029
AP, mm Hg	78.4±2.52	72.6±1.72	0.094
LVP, mm Hg	91.1±3.53	85.9±2.08	0.244
EDP, mm Hg	11.7±1.3	18.4±2.24	0.0218
+dP/dt, mm Hg/s	4459±243	3636±178	0.0226
−dP/dt, mm Hg/s	−5547±352	−4129±202	0.0067

LVEDd indicates LV end-diastolic internal diameter; LVESd, LV end-systolic internal diameter; IVS, interventricular septal thickness; LVPW, LV posterior wall thickness; LVFS, LV fractional shortening; HR, heart rate; CVP, central venous pressure; AP, mean blood pressure; LVP, peak LV pressure; EDP, LV end-diastolic pressure; +dP/dt, maximum dP/dt; and −dP/dt, minimum dP/dt.

Result are expressed as mean±SEM.

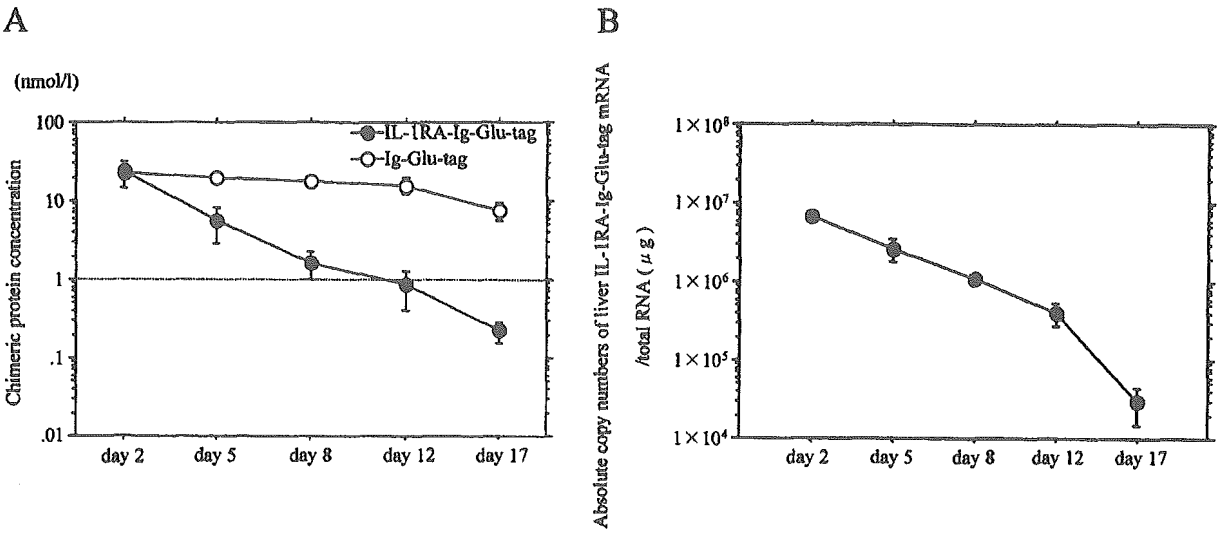

Figure 2. A, Plasma IL-1RA-Glu-tag protein and Ig-Glu-tag protein levels. Chimeric protein concentrations were calculated by use of Glu-tag. B, Absolute copy numbers of IL-1RA mRNA in liver (n=4). Error bars represent SEM. IL-1RA-Ig-Glu-tag indicates rats injected with pCAGGS-mouse IL-1RA-Ig-Glu-tag; Ig-Glu-tag, rats injected with pCAGGS-rat SP-Ig-Glu-tag.

to increase, peaking at 22.75±2.34 nmol/L on day 2, and gradually decrease to 19.48±1.62 nmol/L on day 5, 17.50±2.50 nmol/L on day 8, 15.59±3.56 nmol/L on day 12, and 7.45±1.88 nmol/L on day 17 (Figure 2A). The expressions of IL-1RA-Ig-Glu-tag transferred into normal rat liver by hydrodynamics-based gene delivery were similar to plasma IL-1RA-Ig-Glu-tag protein levels (Figure 2B). It has been reported that IL-1RA (1 to 10 ng/mL, 0.05 to 0.5 nmol/L) suppresses the production of PGES from rat astrocytes stimulated by lipopolysaccharide in vitro.[28] These results indicated that continuous effective delivery of IL-1RA-Ig protein for >16 days can be achieved in rats by hydrodynamics-based transfection.

Gene Expression of IL-1 Family in Purified Cells From EAM Hearts

Both IL-1α and IL-1β were strongly expressed in CD11b$^+$ cells. The IL-1RI gene was strongly expressed in NCNI cells (the cell fraction containing mainly fibroblasts, smooth muscle cells, and endothelial cells) and $\alpha\beta$T cells, whereas the IL-1RII gene was found to be markedly expressed in CD11b$^+$ cells. The IL-1Racp gene was strongly expressed in both CD11b$^+$ and NCNI cells and was moderately expressed in $\alpha\beta$T cells. Both total IL-1RA and sIL-1RA were detected in CD11b$^+$ cells. These results suggested that IL-1, produced mainly by CD11b$^+$ cells, acted on NCNI and $\alpha\beta$T cells by binding to IL-1RI and transduced intracellular signals by forming with IL-1Racp. On the other hand, CD11b$^+$ cells also produced native IL-1RA and IL-1RII, potentially suppressing the action of IL-1 (Figure 3).

Expression of Immunologic Molecules in Cultivated Cells With Serum Containing IL-1RA-Ig

IL-1RA-Ig–containing serum significantly reduced expression of PGES (mean±SEM, 1.22±0.22 versus 1.94±0.17; P<0.0001), Cox-2 (0.93±0.24 versus 2.00±1.05; P=0.0092), and IL-1β (3.91±1.22 versus 11.25±2.16; P<0.0001) at the mRNA level in cultivated NC cells (the cell fraction containing mainly fibroblasts, smooth muscle cells, and CD11b$^+$ cells) (Figure 4). In addition, IL-1RA-Ig–containing serum significantly reduced expression of the IL-2 (0.0004±0.0001 versus 0.0310±0.0090; P<0.0001) and IFN-γ (0.0065±0.0036 versus 0.0461±0.0385; P=0.0091) genes in cultivated lymphocytes (Figure 5).

Discussion

In the present study, we demonstrated that hydrodynamics-based delivery of plasmid DNA encoding the IL-1RA-Ig gene ameliorated EAM. IL-1RA-Ig–affecting cells were thought to be NCNI cells (fibroblasts, smooth muscle cells, and endothelial cells) and $\alpha\beta$T cells because IL-1RI and IL-1Racp were found in them. Endogenous IL-1α and IL-1β produced mainly by CD11b$^+$ cells, especially secreted IL-1β, influence these surrounding cells in a paracrine manner. IL-1RA-Ig, generated after gene transfer, appears to inhibit the IL-1–induced reactions of these cells and ameliorates EAM.

The functions of IL-1 with respect to cell regulation are varied.[29] In this study, the effect of serum containing IL-1RA-Ig on the mRNA expression of various immunologic molecules in cultivated NC cells (mainly fibroblasts, smooth muscle cells, and CD11b$^+$ cells) from hearts and lymphocytes from popliteal lymph nodes of EAM rats was investigated. The concentration of IL-1RA-Ig in cultivated cells was almost the same as that observed at the onset of myocarditis (day 10 to 11) and that reported by previous in vitro studies to be an effective dose.[28,30] In this study, there was a 30- to 50-fold increase in the expression of PGES, Cox-2, and IL-1β mRNA in NC cells by IL-1 alone, but the increase was significantly reduced by serum containing IL-1RA-Ig. PGE2 produced by PGES plays an important role in inflammation and pain.[31] In rheumatoid arthritis, the level of PGES detected

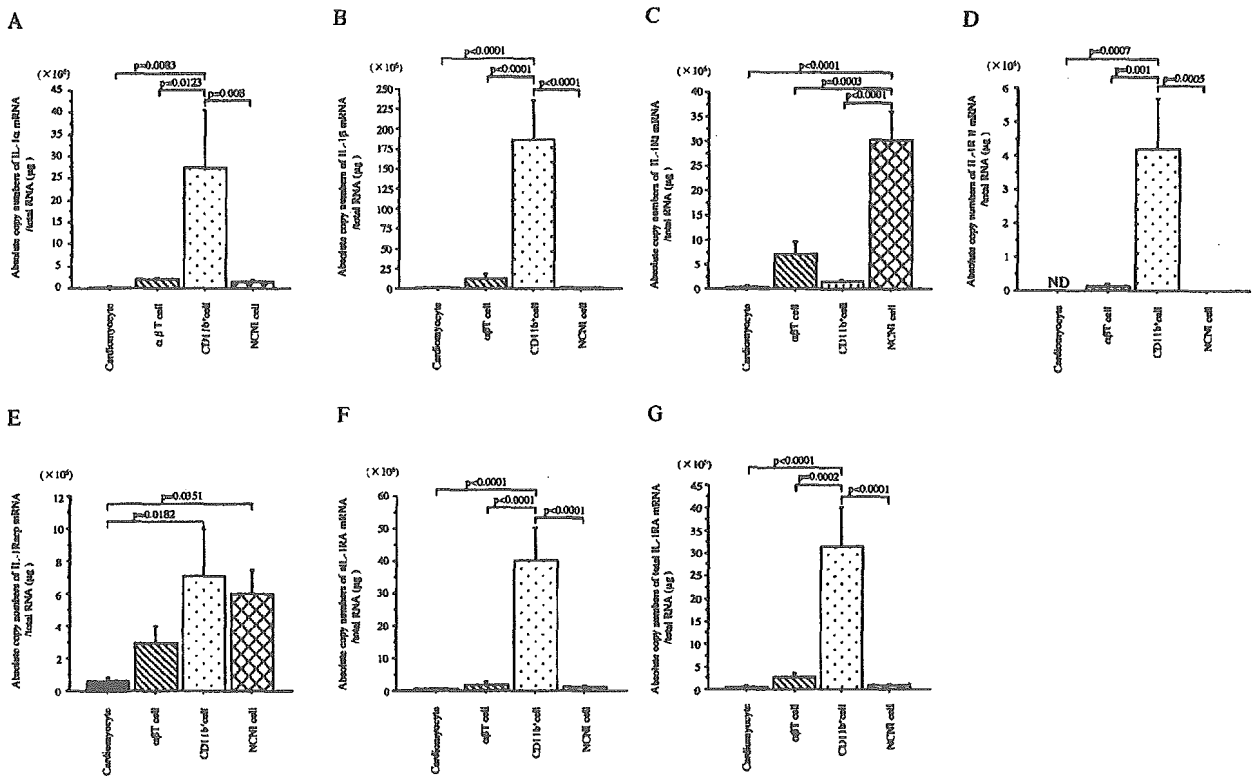

Figure 3. A through G, Absolute copy numbers of IL-1α, IL-1β, IL-1RI, IL-1RII, IL-1Racp, sIL-1RA, and total IL-1RA, respectively. Each cell was separated and purified from EAM heart on day 18. Error bars represent SEM. Statistical assessment was performed by 1-way ANOVA and Bonferroni multiple comparison test. Differences were considered significant at $P<0.05$.

at the inflammatory region is very high.[32] Our study of PGES and Cox-2 gene expression in purified cells from EAM hearts indicated that they were produced mainly by NCNI cells and slightly by CD11b$^+$ cells (data not shown). IL-1RA-Ig may inhibit the expression of the PGES and Cox-2 gene directly on NCNI cells via IL-1R. IL-1–induced IL-1 production has been shown in various cell types.[33] IL-1RA-Ig may also inhibit IL-1 production directly on NCNI cells. However, because our study indicated that IL-1 was produced mainly by CD11b$^+$ cells, IL-1RA-Ig may inhibit IL-1 production of CD11b$^+$ cells indirectly via NCNI cells or $\alpha\beta$T cells. Reduced PGES, Cox-2, and/or IL-1 production by NC cells in EAM hearts may be an effect resulting in improved myocarditis. On the other hand, in lymphocytes of popliteal lymph node, IL-2 and IFN-γ mRNA expression levels were significantly reduced by serum containing IL-1RA-Ig. In EAM,

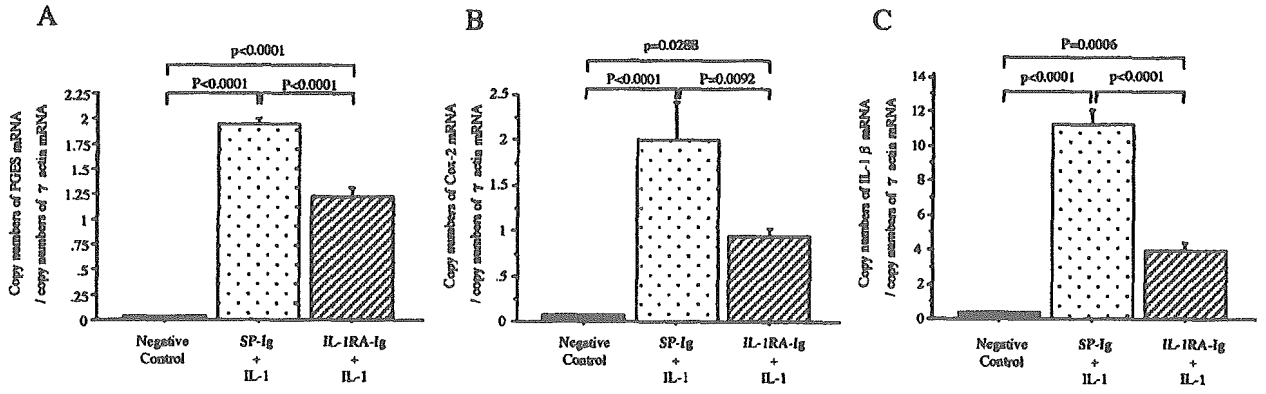

Figure 4. Copy numbers of various immunologic molecules mRNA/copy numbers of γ-actin mRNA in NC cells cultivated from EAM hearts. A, PGES; B, Cox-2; C, IL-1β. Negative control cells were cultivated in medium without IL-1α and rat serum. SP-Ig+IL-1 cells were cultivated in medium with IL-1α and rat serum treated with pCAGGS-SP-Ig-Glu-tag; IL-1RA-Ig+IL-1 cells were cultivated in medium with IL-1α and rat serum treated with pCAGGS-mouse IL-1RA-Ig-Glu-tag. Error bars represent SEM. Statistical assessment was performed by 1-way ANOVA and Bonferroni multiple comparison test. Differences were considered significant at $P<0.05$.

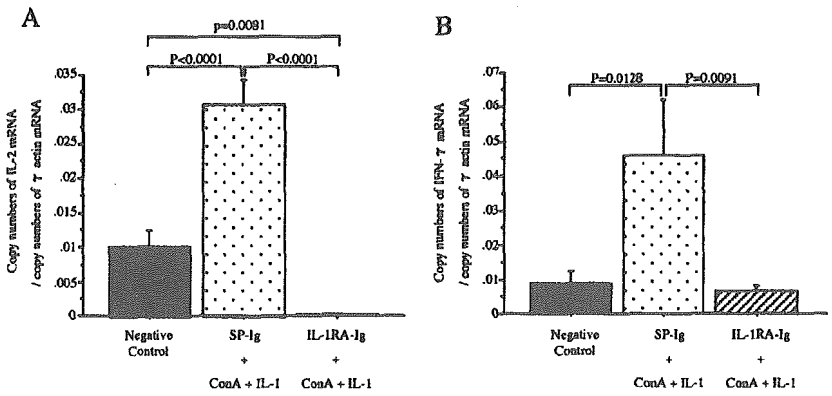

Figure 5. Copy numbers of various immunologic molecules mRNA/copy numbers of γ-actin mRNA in cultivated lymphocytes from swollen lymph node of EAM. A, IL-2; B, IFN-γ. Negative control cells were cultivated in medium without Con-A, IL-1α, and serum. SP-Ig+Con-A+IL-1 cells were cultivated in medium with Con-A, IL-1α, and rat serum treated with pCAGGS-SP-Ig-Glu-tag. IL-1RA-Ig+Con-A+IL-1 cells were cultivated in medium with Con-A, IL-1α, and rat serum treated with pCAGGS-mouse IL-1RA-Ig-Glu-tag. Error bars represent SEM. Statistical assessment was performed by 1-way ANOVA and Bonferroni multiple comparison test. Differences were considered significant at $P<0.05$.

which is a T cell–mediated disease,[27] Th1 cytokines such as IL-2 and IFN-γ produced by $CD4^+$ T cells are thought to play a central role.[4] Therefore, inhibition of Th1 cytokine production by IL-1RA-Ig may improve EAM.

In human rheumatoid arthritis, it has been reported that Anakinra (a recombinant form of IL-1RA) suppressed progression of this disease,[34] and treatment with IL-1RA has been investigated in various animal models.[16–18] Therefore, the number of diseases in which IL-1RA has a therapeutic relevance may be extended in the near future. Human myocarditis is serious and often fatal despite intensive care. However, the cause of myocarditis is not usually evident. It was reported that gene therapy with IL-1RA expression plasmid was effective in the treatment of viral myocarditis and reduced virus titer in hearts.[18] Here, we demonstrated that IL-1RA-Ig gene transfer ameliorated EAM resembling human giant cell myocarditis. Therefore, treatment with IL-1RA may be effective for acute and fulminant myocarditis even if its cause is unknown.

Hydrodynamics-based gene delivery of plasmid DNA as used in this study is both inexpensive and highly effective in terms of facilitating gene expression. The concentration of IL-1RA-Ig in blood obtained by this method was higher compared with plasmid DNA transfection into muscle with in vivo electroporation.[19,20] The producing cells to which plasmid DNA is transferred by this method are thought to be mainly hepatocytes. Plasmid DNA is thought to be delivered into hepatocytes by retrograde blood flow from hepatic veins. If plasmid DNA encoding IL-1RA-Ig can be directly transfected into the heart, T cells and NCNI cells in EAM hearts will be highly influenced by IL-1RA-Ig, and EAM may be ameliorated. Hou et al[35] reported heart-targeted plasmid DNA transfer by retrograde coronary vein using a balloon catheter. This method, which is easy and not very risky, may be suitable for human clinical application. New developments of this gene therapy can be expected in the future.

References

1. Kodama M, Matsumoto Y, Fujiwara M, Masani F, Izumi T, Shibata A. A novel experimental model of giant cell myocarditis induced in rats by immunization with cardiac myosin fraction. *Clin Immunol Immunopathol.* 1990;57:250–262.
2. Kodama M, Hanawa H, Saeki M, Hosono H, Inomata T, Suzuki K, Shibata A. Rat dilated cardiomyopathy after autoimmune giant cell myocarditis. *Circ Res.* 1994;75:278–284.
3. Kodama M, Zhang S, Hanawa H, Shibata A. Immunohistochemical characterization of infiltrating mononuclear cells in the rat heart with experimental autoimmune giant cell myocarditis. *Clin Exp Immunol.* 1992;90:330–335.
4. Hanawa H, Abe S, Hayashi M, Yoshida T, Yoshida K, Shiono T, Fuse K, Ito M, Tachikawa H, Kashimura T, Okura Y, Kato K, Kodama M, Maruyama S, Yamamoto T, Aizawa Y. Time course of gene expression in rat experimental autoimmune myocarditis. *Clin Sci (Lond).* 2002;103: 623–632.
5. March CJ, Mosley B, Larsen A, Cerretti DP, Braedt G, Price V, Gillis S, Henney CS, Kronheim SR, Grabstein K. Cloning, sequence and expression of two distinct human interleukin-1 complementary DNAs. *Nature.* 1985;315:641–647.
6. Scala G, Allavena P, Djeu JY, Kasahara T, Ortaldo JR, Herberman RB, Oppenheim JJ. Human large granular lymphocytes are potent producers of interleukin-1. *Nature.* 1984;309:56–59.
7. Rupp EA, Cameron PM, Ranawat CS, Schmidt JA, Bayne EK. Specific bioactivities of monocyte-derived interleukin 1 alpha and interleukin 1 beta are similar to each other on cultured murine thymocytes and on cultured human connective tissue cells. *J Clin Invest.* 1986;78:836–839.
8. Baldari C, Murray JA, Ghiara P, Cesareni G, Galeotti CL. A novel leader peptide which allows efficient secretion of a fragment of human interleukin-1 beta in Saccharomyces cerevisiae. *EMBO J.* 1987;6: 229–234.
9. Sims JE, Acres RB, Grubin CE, McMahan CJ, Wignall JM, March CJ, Dower SK. Cloning the interleukin 1 receptor from human T cells. *Proc Natl Acad Sci U S A.* 1989;86:8946–8950.
10. Wesche H, Korherr C, Kracht M, Falk W, Resch K, Martin MU. The interleukin-1 receptor accessory protein (IL-1RAcP) is essential for IL-1–induced activation of interleukin-1 receptor–associated kinase (IRAK) and stress-activated protein kinases (SAP kinases). *J Biol Chem.* 1997;272:7727–7731.
11. Colotta F, Re F, Muzio M, Bertini R, Polentarutti N, Sironi M, Giri JG, Dower SK, Sims JE, Mantovani A. Interleukin-1 type II receptor: a decoy target for IL-1 that is regulated by IL-4. *Science.* 1993;261:472–475.
12. Arend WP, Malyak M, Guthridge CJ, Gabay C. Interleukin-1 receptor antagonist: role in biology. *Annu Rev Immunol.* 1998;16:27–55.
13. McIntyre KW, Stepan GJ, Kolinsky KD, Benjamin WR, Plocinski JM, Kaffka KL, Campen CA, Chizzonite RA, Kilian PL. Inhibition of interleukin-1 (IL-1) binding and bioactivity in vitro and modulation of acute inflammation in vivo by IL-1 receptor antagonist and anti-IL-1 receptor monoclonal antibody. *J Exp Med.* 1991;173:931–939.
14. Dinarello CA. The interleukin-1 family: 10 years of discovery. *FASEB J.* 1994;8:1314–1325.
15. Guo C, Dower SK, Holowka D, Baird B. Fluorescence resonance energy transfer reveals interleukin (IL)-1–dependent aggregation of IL-1 type I receptors that correlates with receptor activation. *J Biol Chem.* 1995;270: 27562–27568.
16. Badovinac V, Mostarica-Stojkovic M, Dinarello CA, Stosic-Grujicic S. Interleukin-1 receptor antagonist suppresses experimental autoimmune encephalomyelitis (EAE) in rats by influencing the activation and proliferation of encephalitogenic cells. *J Neuroimmunol.* 1998;85:87–95.
17. Kim JM, Jeong JG, Ho SH, Hahn W, Park EJ, Kim S, Yu SS, Lee YW, Kim S. Protection against collagen-induced arthritis by intramuscular gene therapy with an expression plasmid for the interleukin-1 receptor antagonist. *Gene Ther.* 2003;10:1543–1550.

18. Nakano A, Matsumori A, Kawamoto S, Tahara H, Yamato E, Sasayama S, Miyazaki JI. Cytokine gene therapy for myocarditis by in vivo electroporation. *Hum Gene Ther.* 2001;12:1289–1297.
19. Maruyama H, Higuchi N, Nishikawa Y, Kameda S, Iino N, Kazama JJ, Takahashi N, Sugawa M, Hanawa H, Tada N, Miyazaki J, Gejyo F. High-level expression of naked DNA delivered to rat liver via tail vein injection. *J Gene Med.* 2002;4:333–341.
20. Liu F, Song YK, Liu D. Hydrodynamics-based transfection in animals by systemic administration of plasmid DNA. *Gene Therapy.* 1999;6: 1258–1266.
21. Jiang J, Yamato E, Miyazaki J. Sustained expression of Fc-fusion cytokine following in vivo electroporation and mouse strain differences in expression levels. *J Biochem (Tokyo).* 2003;133:423–427.
22. Nishino T, Kodaira T, Shin S, Imagawa K, Shima K, Kumahara Y, Yanaihara C, Yanaihara N. Glucagon radioimmunoassay with use of antiserum to glucagon C-terminal fragment. *Clin Chem.* 1981;27: 1690–1697.
23. Hanawa H, Watanabe R, Hayashi M, Yoshida T, Abe S, Komura S, Liu H, Elnaggar R, Chang H, Okura Y, Kato K, Kodama M, Maruyama H, Miyazaki J, Aizawa Y. A novel method to assay proteins in blood plasma after intravenous injection of plasmid DNA. *Tohoku J Exp Med.* 2004; 202:155–161.
24. Hwang TC, Horie M, Nairn AC, Gadsby DC. Role of GTP-binding proteins in the regulation of mammalian cardiac chloride conductance. *J Gen Physiol.* 1992;99:465–489.
25. Isenberg G, Klockner U. Calcium tolerant ventricular myocytes prepared by preincubation in a "KB medium." *Pflugers Arch.* 1982;395:6–18.
26. Toba K, Hanawa H, Fuse I, Sakaue M, Watanabe K, Uesugi Y, Higuchi W, Takahashi M, Aizawa Y. Difference in CD22 molecules in human B cells and basophils. *Exp Hematol.* 2002;30:205–211.
27. Kodama M, Matsumoto Y, Fujiwara M. In vivo lymphocyte-mediated myocardial injuries demonstrated by adoptive transfer of experimental autoimmune myocarditis. *Circulation.* 1992;85:1918–1926.
28. Pistritto G, Ciabattoni G, Mancuso C, Tringali G, Preziosi P, Navarra P. Signaling pathways involved in lipopolysaccharide stimulation of prostaglandin production by rat hypothalamic astroglial cells. *J Endotoxin Res.* 2000;6:307–311.
29. Dinarello CA. Interleukin-1 and interleukin-1 antagonism. *Blood.* 1991; 77:1627–1652.
30. Rambaldi A, Torcia M, Dinarello CA, Barbui T, Cozzolino F. Modulation of cell proliferation and cytokine production in AML by recombinant interleukin-1 receptor antagonist. *Leukemia.* 1993;7:S10–S12.
31. Trebino CE, Stock JL, Gibbons CP, Naiman BM, Wachtmann TS, Umland JP, Pandher K, Lapointe JM, Saha S, Roach ML, Carter D, Thomas NA, Durtschi BA, McNeish JD, Hambor JE, Jakobsson PJ, Carty TJ, Perez JR, Audoly LP. Impaired inflammatory and pain responses in mice lacking an inducible prostaglandin E synthase. *Proc Natl Acad Sci U S A.* 2003;100:9044–9049.
32. Stichtenoth DO, Thoren S, Bian H, Peters-Golden M, Jakobsson PJ, Crofford LJ. Microsomal prostaglandin E synthase is regulated by proinflammatory cytokines and glucocorticoids in primary rheumatoid synovial cells. *J Immunol.* 2001;167:469–474.
33. Warner SJ, Auger KR, Libby P. Human interleukin 1 induces interleukin 1 gene expression in human vascular smooth muscle cells. *J Exp Med.* 1987;165:1316–1331.
34. Fleischmann RM. Addressing the safety of anakinra in patients with rheumatoid arthritis. *Rheumatology (Oxford).* 2003;42:ii29–ii35.
35. Hou D, Maclaughlin F, Thiesse M, Panchal VR, Bekkers BC, Wilson EA, Rogers PI, Coleman MC, March KL. Widespread regional myocardial transfection by plasmid encoding Del-1 following retrograde coronary venous delivery. *Catheter Cardiovasc Interv.* 2003;58:207–211.

ELSEVIER

Cardiovascular Research 68 (2005) 278 – 288

Cardiovascular Research

www.elsevier.com/locate/cardiores

Expression of immunological molecules by cardiomyocytes and inflammatory and interstitial cells in rat autoimmune myocarditis

Tsuyoshi Yoshida, Haruo Hanawa *, Ken Toba, Hiroshi Watanabe, Ritsuo Watanabe, Kaori Yoshida, Satoru Abe, Kiminori Kato, Makoto Kodama, Yoshifusa Aizawa

Division of Cardiology, Niigata University Graduate School of Medical and Dental Science, 1-754 Asahimachi, Niigata City, 951-8510, Japan

Received 2 November 2004; received in revised form 18 May 2005; accepted 13 June 2005
Available online 12 July 2005
Time for primary review 36 days

Abstract

Background: In a heart with myocarditis, there are cardiomyocytes, inflammatory cells, and non-inflammatory interstitial cells. Immunological molecules are thought to influence not only inflammatory cells but also cardiac function and remodeling. Whatever their origin, the cells they target and the intercellular crosstalk they mediate remain unclear. Here, we examined native gene expression of immunological molecules in normal and rat experimental autoimmune myocarditis (EAM) 18 and 90 days after immunization, using real time RT-PCR in cardiomyocytes, $CD11b^+$ cells, αβT cells and non-cardiomyocytic non-inflammatory (NCNI) cells.

Methods and results: Cells were isolated by collagenase perfusion on a Langendorff apparatus and purified by passing through a stainless-steel sieve followed by magnetic bead column separation using appropriate monoclonal antibodies. Most immunological molecules were expressed in inflammatory cells. However, some were expressed in NCNI cells or cardiomyocytes. Interestingly, most of interleukin (IL)-10, monocyte chemoattractant protein (MCP)-1, or tumor necrosis factor (TNF)-α receptor were found in NCNI cells and most of fractalkine were found in NCNI cells and cardiomyocytes. Moreover, TNF-α significantly upregulated fractalkine and MCP-1 mRNA in cultivated cells from EAM hearts.

Conclusion: In the rat experimental myocarditis heart, inflammatory cells express many immunological molecules. Some of them are thought to influence NCNI cells or cardiomyocytes directly via receptors on these cell types. It is further suggested that fractalkine, IL-10, and MCP-1 expressed in NCNI cells or cardiomyocytes regulate inflammatory cells.

Keywords: Myocarditis; Dilated cardiomyopathy; Autoimmunity; Chemokines; Cytokines; Quantitative RT-PCR

1. Introduction

Rat experimental autoimmune myocarditis (EAM) resembles human giant cell myocarditis [1] and recurrent forms lead to dilated cardiomyopathy (DCM) [2]. $CD4^+$αβT cells play important roles in initiating the disease process, while macrophages and $CD4^+$αβT cells infiltrate the heart during the acute phase [3,4]. Gene expression of immunological molecules in EAM heart changes diversely from acute phase to recovery phase [5]. For example, Th1 cytokine increases in the acute phase and decreases during the recovery phase. On the other hand, Th2 cytokine increases during the recovery phase [5,6]. Immunological molecules, in addition to their influence on inflammatory cells, are believed also to affect cardiac function and mediate myocardial damage [7]. It is thought that inflammatory cells and non-inflammatory cells in EAM heart engage in crosstalk by means of immunological molecules. Thus far, in vivo analysis of immunological molecules and their receptor-expressing origin cells has not been performed satisfactorily. It is important to determine which cells express these molecules or their ligands and receptors in order to understand deterioration of cardiac function and remodeling in myocarditis.

* Corresponding author. Tel.: +81 25 227 2185; fax: +81 25 227 0774.
E-mail address: hanawa@med.niigata-u.ac.jp (H. Hanawa).

0008-6363/$ - see front matter © 2005 European Society of Cardiology. Published by Elsevier B.V. All rights reserved.
doi:10.1016/j.cardiores.2005.06.006

In this study, we investigated native gene expression of immunological molecules by using real time RT-PCR in cardiomyocytes, αβT cells, $CD11b^+$ cells (macrophages/granulocytes/dendritic cells in part) or non-cardiomyocytic non-inflammatory (NCNI) cells without cultivation. Cells were isolated and purified by passing through a stainless-steel sieve and using appropriate monoclonal antibodies on a magnetic bead column separation system. Moreover, we examined the effect of tumor necrosis factor (TNF)-α on immunological molecules in cultivated cells from EAM hearts. We aimed to elucidate implications on the potential crosstalk in EAM.

2. Methods

2.1. Animals

Lewis rats were obtained from Charles River, Japan (Atsugi, Kanagawa, Japan) and were maintained in our animal facilities until they reached 7 weeks of age. Throughout the studies, all the animals were treated in accordance with the guidelines for animal experiments of our institute and the guide for the care and use of laboratory animals published by the US National Institutes of Health.

2.2. Induction of EAM

Whole cardiac myosin was prepared from the ventricular muscle of porcine hearts as previously described [1]. It was dissolved in PBS at a concentration of 10 mg/ml and emulsified with an equal volume of complete Freund's adjuvant supplemented with 10 mg/ml of *Mycobacterium tuberculosis* H37RA (Difco, Detroit, Michigan). On day 0, the rats received a single immunization at 2 subcutaneous sites with a total of 0.2 ml of emulsion for each rat. Normal rats ($n=5$), EAM rats were killed on day 18 ($n=6$) (acute phase), and EAM rats were killed on day 90 ($n=6$) (chronic phase).

2.3. Isolation of cells, flow cytometric analysis and cell purification

Cardiomyocytes and non-cardiomyocytes in hearts of normal and myocarditis rats on days 18 and 90 were isolated after collagenase perfusion treatment for 15–20 min using a Langendorff apparatus as reported previously [8,9]. Isolated cells in an isotonic buffer were separated serially through a 38 μm stainless-steel sieve twice and a 20 μm stainless-steel sieve twice. Cells larger than 38 μm and smaller than 20 μm were considered as cardiomyocytes and non-cardiomyocytes, respectively (Fig. 1). The cell fraction between 20 and 38 μm consisted of both cell types and was therefore discarded. The number of non-cardiomyocytes recovered from normal hearts was very small but the number from myocarditis hearts on day 18 was sufficient for statistically significant analysis. Phenotype was analyzed in both samples and cell purification was performed only in samples obtained from myocarditis hearts on day 18.

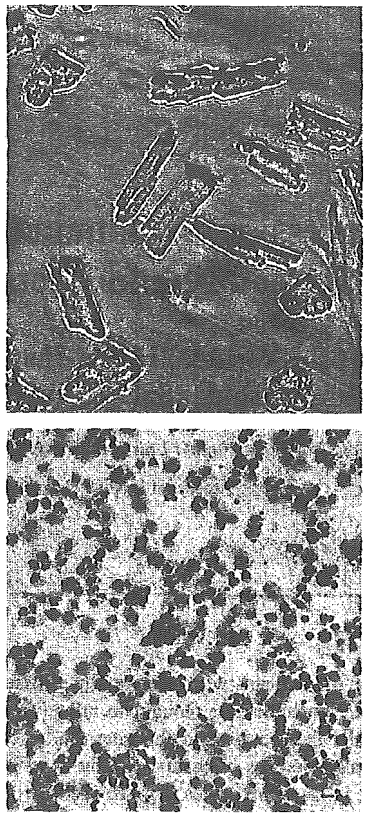

Fig. 1. Microscopic findings. (A) Cardiomyocytes which were not passed through 38 μm stainless-steel sieve twice. (B) Non-cardiomyocytes which were passed through 20 μm stainless-steel sieve twice. May–Giemsa staining. Bar represents 10 μm.

Phycoerythrin (PE)-conjugated mouse monoclonal antibodies against rat CD8 (clone OX-8) and CD25 (OX-39) were purchased from Immunotech, Marseille, France. PE-conjugated anti-CD3 (G4.18), CD4 (OX-35), TCRαβ (R73), CD161 (10/78), CD11b (OX-42), and biotinylated anti-TCRγ/δ were purchased from Pharmingen, San Diego, CA. Biotinylated ED1 and PE-conjugated streptavidin (SA–PE) were purchased from Serotec, Oxford, UK, and Becton Dickinson, San Jose, CA, respectively. Cells suspended in 50% rat serum in a buffer were directly stained with a PE-conjugated monoclonal antibody or serially stained with a biotinylated monoclonal antibody and SA–PE, then analyzed using a FACScan flow cytometer (Becton Dickinson).

$TCR\alpha/\beta^+$T cells, $TCR\alpha/\beta^-/CD11b^+$ cells, and $TCR\alpha/\beta^-/CD11b^-$ cells (NCNI cells) were sorted using PE-conjugated monoclonal antibodies, anti-PE micro beads (Miltenyi Biotec, Bergisch Gladbach, Germany) and a MACS magnetic cell sorting system (Miltenyi Biotech) [10]. In brief, cells were serially labeled with PE-conjugated anti-TCRα/β and anti-PE micro beads and separated with a MS column in a

magnetic field. The positive fraction was further purified using another MS column (purity, 99.4±0.5%, $n=3$). Contaminated cells in the negative fraction were removed using a LD column and utilized for the succeeding sorting. The TCRα/β$^-$ cells were serially labeled with PE-conjugated anti-CD11b and anti-PE micro beads, then separated with a MS column in a magnetic field. The positive fraction was further purified using another MS column (purity, 97.0±2.3%, $n=3$). Contaminated cells in the negative fraction were removed using a LD column (final contamination of positive cells, 2.2±1.1%, $n=3$, Fig. 2).

2.4. Immunostaining

Cytospin preparations of purified cell fractions were made and slides were stained with May–Giemsa stain or

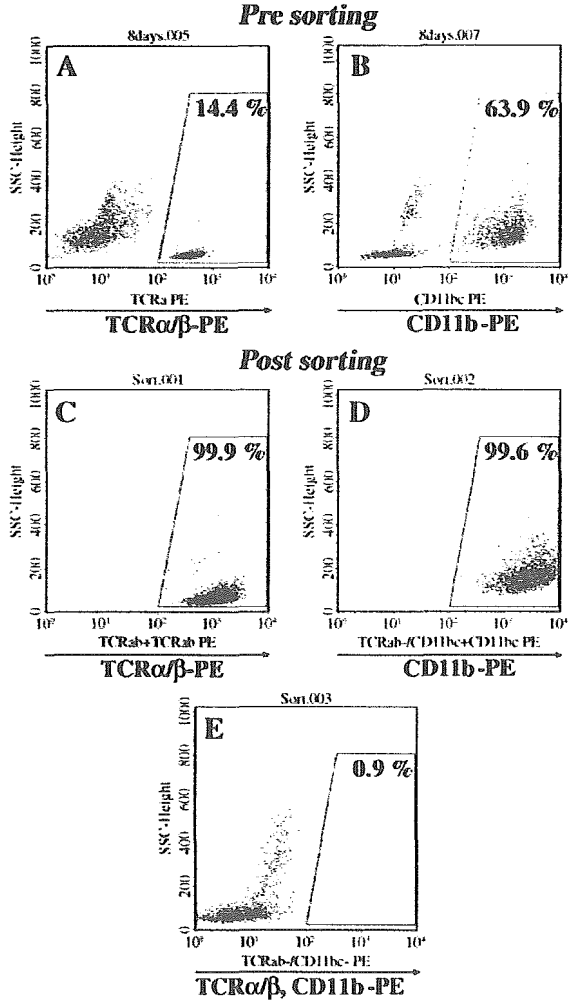

Fig. 2. Purification quality of non-cardiomyocytes. (A and B) Before sorting. (C–E) Sorted cells of TCRα/β$^+$, TCRα/β$^-$/CD11b$^+$ and TCRα/β$^-$/CD11b$^-$, respectively. Vertical axis and horizontal axis, side scattergram and PE-fluorescence, respectively. The results are representative of studies with three separate myocarditis rats on day 18.

naphthol AS-D chloroacetate esterase and α-naphthylbutyrate esterase stain. Cytospin slides prepared from NCNI cell fraction were immunostained with mouse monoclonal anti-α smooth muscle actin antibodies (SIGMA, Saint Louis, MO), rabbit anti-Factor VIII related antigen antibodies (Zymed Laboratories, San Francisco, CA) and rabbit anti-rat collagen III antibodies (Monosan, Uden, Netherlands). Sections were incubated for 60 min at 37 °C in a humidified chamber with this antibody. The slides were washed in TBS three times. Immunodetection was performed using biotinylated anti-rabbit and anti-mouse immunoglobulins followed by alkaline phosphatase conjugated streptavidin and a Fast Red chromogen (kit LSAB2; DAKO Corp., Carpinteria, CA) for red staining. The sections were lightly counterstained with Mayer's hematoxylin. Negative control slides were incubated with either mouse IgG2a or normal rabbit serum instead of the primary antibody. Sections of EAM heart were stained with hematoxylin and eosin stain. For immunostaining of OPN, paraffin sections of EAM heart on day 18 were cut at 6 μm, deparaffinized with xylene, hydrated with decreasing concentrations of ethanol and heated in a hot water bath for 40 min at 95 °C in ChemMate Target retrieval solution (Daco Corp.). The sections were probed with rabbit anti-human OPN polyclonal antibody (1:50 dilution; IBL, Gunma, Japan) for 60 min in a humidified chamber. After several washings with TBS, immunodetection was performed using biotinylated anti-rabbit and anti-mouse immunoglobulins followed by alkaline phosphatase conjugated streptavidin and a Fast Red chromogen. The sections were lightly counterstained with Mayer's hematoxylin.

2.5. RNA isolation from heart and reverse transcription

We prepared 1 to 5×10^6 purified cells and total RNA was isolated from each purified cell fraction (cardiomyocytes; $n=5$, CD11b$^+$ cells; $n=5$, αβT cells; $n=5$ and NCNI cells; $n=6$) of EAM hearts on day 18 (acute phase) after immunization and from each cardiomyocytes fraction of normal hearts ($n=5$) and EAM hearts on day 90 (chronic phase $n=6$) using Trizol (LifeTechnologies, Tokyo, Japan) [5]. To confirm that gene expression of cardiomyocytes after collagenase preparation is similar to native cardiomyocytes, we prepared purified cardiomyocytes ($n=4$) and whole heart ($n=4$), which are homogenated immediately in Trizol, on days 0, 14, 21 and 28 and then total RNA was isolated from each sample. cDNA was synthesized from 2–5 μg of total RNA with random primers and murine Moloney leukemia virus reverse transcriptase in a final volume of 20 μl.

2.6. Plasmid construction as standard sample for real time RT-PCR

Immunological molecules and specific marker cDNAs were amplified with AmpliTaq polymerase (TOYOBO,

Osaka, Japan), for each primer (Table 1) from 1 μl of cDNA according to the following amplification protocol: 35 cycles at 94 °C for 60 s, 58 °C for 90 s, and 73 °C for 120 s. Amplified cDNAs were directly inserted into the pGEM-T easy vector and the recombinant plasmids were isolated after transforming with *Escherichia coli* JM109 competent cells using the MagExtractor plasmid kit (TOYOBO, Osaka, Japan). The plasmids were diluted with DNAse-free water in a siliconised tube including 10 ng/μl MS2 RNA (Roche, Indianapolis, IN) to prevent adherence to the tube wall.

2.7. Quantitative RT-PCR

cDNA was diluted 100-fold with DNAse-free water in a siliconised tube (including 10 ng/μl MS2 RNA to prevent adherence to the tube wall) and 5 μl was then used for real-time PCR. cDNA and diluted plasmid were amplified with the same primer used for making the plasmid and LightCycler-FastStart DNA Master SYBR Green I (Roche, Indianapolis, IN). RNAs without reverse transcription were used as a negative control. After an initial denaturation step of 10 min at 95 °C, a three-step cycle procedure was used (denaturation 95 °C, 10 s, annealing 62–65 °C, 10 s and extension 72 °C, 13 s) for 40 cycles. The LightCycler Software calculated a standard curve using five plasmid standards. The standard curve was created by plotting the cycle numbers at which the fluorescent signals entered the log-linear phase vs the concentrations of the standards. The absolute copy numbers of all the samples were calculated by the LightCycler software using this standard curve [5].

Table 2
Absolute copy number of mRNA/microgram of total RNA

	Cultivated NC cells ($n=6$)
α cardiac myosin	N.D.
CD3	N.D.
CD11b	2,470,000±1,460,000
von Willebrand factor	531,000±161,000
Collagen type III	470,000,000±158,000,000
Calponin	13,500,000±8,380,000
TNF-α receptor	66,000,000±40,500,00

Results are expressed as the mean±SEM. N.D.; not detected.

2.8. Non-cardiomyocytic cell culture with TNF-α

On day 18, non-cardiomyocytic (NC) cells were isolated from the hearts of EAM rats via collagenase preparation and were cultured for three weeks on 35-mm well dishes in 2 ml of RPMI medium supplemented with 10% FCS. These cultivated NC cells were suggested to contain mainly fibroblasts, smooth muscle cells, endothelial cells and $CD11b^+$ cells and to express enough mRNA of TNF-α receptor, as determined by gene expression analysis (Table 2). After reaching confluency, NC cells were stimulated by adding TNF-α (Pepro Tech, London, England) (no TNF-α group, $n=6$; 80 ng/ml of TNF-α group, $n=6$; and 160 ng/ml of TNF-α group, $n=6$). After culture for 24 h at 37 °C, NC

Table 1
List of primers

	Sense primer	Antisense primer
α cardiac myosin	5′-acaaggttaaaaacctgacagagg-3′	5′-tactgttctgctgctgctgtcaa-3′
β cardiac myosin	5′-cactccagaagagaagaactccat-3′	5′-ccagttgaacatcttctcgtacac-3′
ANP	5′-atggatttcaagaacctgctagac-3′	5′-gtccaatcctgtcaatcctac-3′
CD3	5′-gatcccaaactctctatagcta-3′	5′-ctttcatgccaatctcactgtg-3′
CD11b	5′-gggatccgtaaagtagtgagaa-3′	5′-aaaggagctggtacttcctgtct-3′
Collagen type 3	5′-cgcaattgcagagacctgaa-3′	5′-acagtcatgggactggcatttat-3′
vo Willebrand factor	5′-agaggctacatctctcagaag-3′	5′-gaccttcttcttgaaaccttg-3′
Calponin	5′-aacataggaaatttcatcaaagcc-3′	5′-gtagactgatagttgcctgatcca-3′
Caldesmon	5′-atggaagaaacagaagtggtcatc-3′	5′-cctcagctctctctctctctg-3′
IL-2	5′-ctgagagggatcgataattcaaga-3′	5′-attggcactcaaattgttttcag-3′
IFN-γ	5′-atctggaggaactggcaaaaggacg-3′	5′-ccttaggctagattctggtgacagc-3′
INF-γ receptor	5′-aagagtttattatgccgaaagg-3′	5′-tgtattaacttgccagaaagacga-3′
IL-10	5′-actgctatgttgcctgctcttact-3′	5′-gaattcaaatgctcttgatttct-3′
IL-10 receptor	5′-tgacagtgacctagtccagaactc-3′	5′-ttgattccactgtctacttggtgt-3′
TNF α	5′-atgggctccctctcatcagt-3′	5′-actccagctgctcctctgct-3′
TNF α receptor	5′-aaaggaacctacttggtgagtgac-3′	5′-gttacacacggtgttctgtttctc-3′
MCP-1	5′-ctgtctcagccagatgcagttaat-3′	5′-tatgggtcaagttcacxattcaaag-3′
Fractalkine	5′-ctcgccaatcccagtgaccttgctc-3′	5′-gattggtagacagcagcaatcggccaaatg-3′
CX3CR1	5′-agctgctcaggacctcaccat-3′	5′-gttgtggaggccctcatggctgat-3′
MCH Class I	5′-ctctgggaaggagacagaattac-3′	5′-tttcaatctgggagagcacatc-3′
MHC Class II	5′-aaatacttcaggacagttgaaccc-3′	ccgactccactcatcttcttattt-3′
PD-1	5′-cagcaaccagactgaaaaacag-3′	5′-acaatgaccaagccttgaact-3′
PD-1L	5′-gcagattcccagtagaacagaaat-3′	5′-acattagttcagctcagaagtgg-3′
Osteopontin	5′-aacggatgactttaagcaagaaac-3′	5′-tactgttcacagaaacagggaaa-3′
CD44	5′-aacatgcaggatatgggttcatag-3′	5′-tcatctataatgtttgaggcatcg-3′
γ-actin	5′-agccttccttccgggcatggagt-3′	5′-tggaggggcctgactcgtcatact-3′

Table 3
Subpopulations of non-cardiomyocytes in normal (day 0) and myocarditis (day 18) rat hearts

	Day 0 ($n=3$)	Day 18 ($n=5$)
CD3 (%)	7.9±2.4	12.6±2.6
TCR α/β (%)	7.7±2.0	14.1±2.9
TCR γ/δ (%)	0.4±0.1	0.1±0.1
CD161 (%)	11.04±4.3	1.9±0.4
CD4 (%)	4.4±2.8	12.2±2.1
CD8 (%)	8.5±2.1	1.5±0.6
CD25 (%)	0.3±0.2	0.6±02
CD11b (%)	43.4±12.4	64.3±5.3
EDI (5)	30.6±8.2	65.0±4.5

Results are expressed as the mean±SD.

cells were collected and total RNA was isolated as described above. The absolute copy numbers of γ-actin, fractalkine, monocyte chemoattractant protein (MCP)-1 and osteopontin mRNA were measured by quantitative real-time PCR.

2.9. Statistical analysis

Data obtained from quantitative RT-PCR are expressed as mean±standard error of the mean (SEM). Data obtained from flow cytometric analysis are expressed as mean± standard deviation (SD). Differences between groups of purified cells were determined by one-way ANOVA and Bonferroni's multiple comparison test. A value of $P \leq 0.05$ was considered statistically significant.

3. Results

3.1. Flow cytometry of non-cardiomyocytes

The number of $CD4^+\alpha\beta T$ cells and $CD11b^+$ cells increased on day 18 as compared with the control. On day 18, 65% of non-cardiomyocytes were $CD11b^+$ cells and ED-

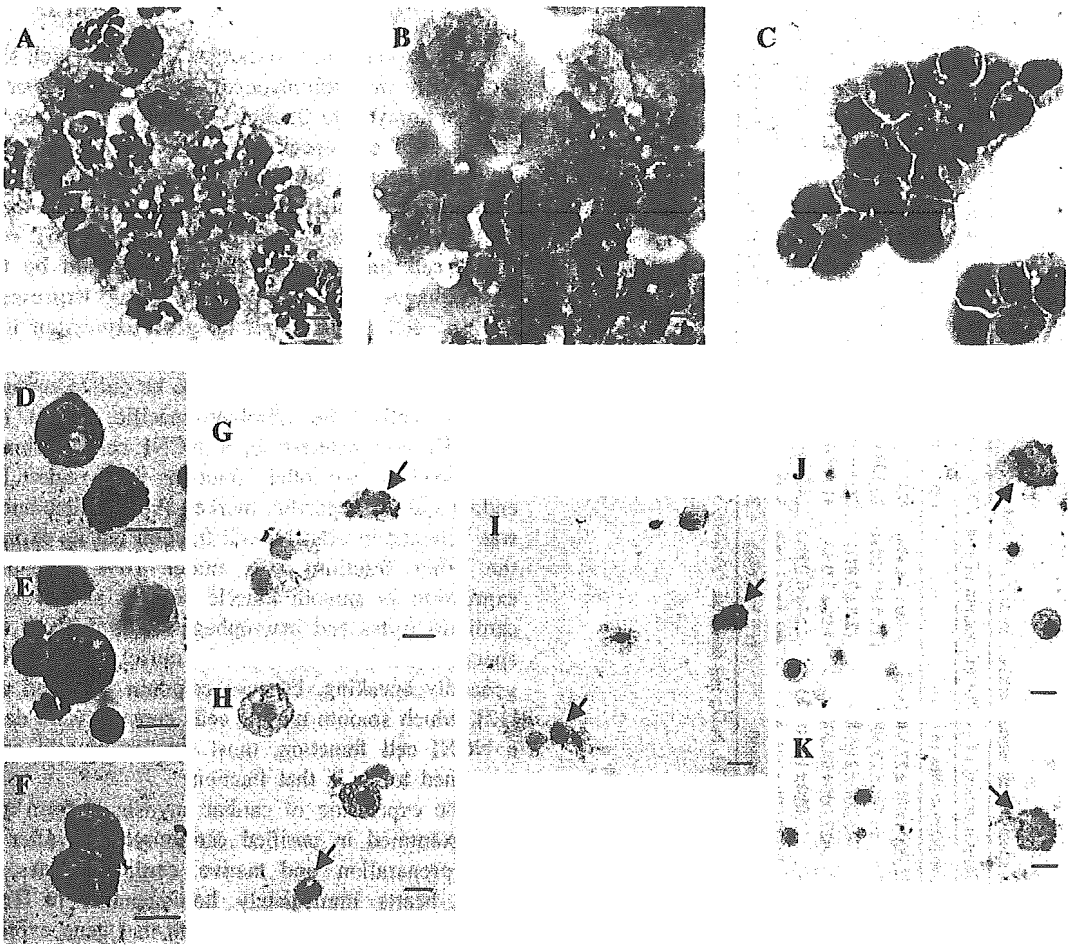

Fig. 3. Purified cells on cytospin slides. (A) $CD11b^+$ cell fraction cells were stained with May–Giemsa stain. (B) $CD11b^+$ cell fraction cells were stained with naphthol AS-D chloroacetate esterase and α-naphthylbutyrate esterase stain. Macrophages were visualized in brown and neutrophilic granulocytes in blue. (C) αβT cell fraction cells were stained with May–Giemsa stain. (D–F) NCNI cell fraction cells were stained with May–Giemsa stain. (G and H) NCNI cell fraction cells were stained with anti-Factor VIII related antigen antibodies. (I) NCNI cell fraction cells were stained with anti-α smooth muscle actin antibodies. (J and K) NCNI cell fraction cells were stained with anti-rat collagen III antibodies. Bar represents 10 μm. Arrows indicate positive staining.

Table 4
Absolute copy numbers of specific cell marker mRNA in day 18 EAM hearts

	Copy numbers of mRNA/microgram of total RNA (copy numbers of mRNA/the most copy numbers of mRNA)							
	Cardiomyocytes ($n=5$)		αβT cells ($n=3$)		$CD11b^+$ cells ($n=5$)		NCNI cells ($n=5$)	
α cardiac myocsin	62,000,000P±27,500,000†	(100±44.4%)	N.D.		N.D.		N.D.	
CD3	65,700±27,500	(0.25±0.10%)	26,300,000±8,840,000†	(100±33.6%)	93,100±28,400	(0.35±0.11%)	1,120,000±346,000	(4.3±1.3%)
CD11b	785,000±219,000	(2.8±0.8%)	2,020±957,000	(7.2±3.4%)	28,000,000±10,800,000†	(100±38.6%)	154,000±85,000	(0.55±0.30%)
von Willebrand factor	487,000±98,800	(9.92±2.0%)	416,000±217,000	(8.5±4.4%)	171,000±28,400	(3.5%±0.58)	4,890,000±1,160,000†	(100±23.7%)
Collagen type III	19,800±1,810,000	(0.54±0.05%)	24,200±11,400	(0.66±.013%)	16,400,000±4,200,000	(0.45±0.11%)	3,660,000,000±472,000,000†	(100±12.9%)
Caponin	1,000,000±285,000	(42.4±12.1%)	N.D.		104,000±86,200	(4.4±3.7%)	2,360,000±594,000*	(100±25.2%)
Caldesmon	21,800±4940	(11.3±2.6%)	24,400±9670	(12.6±5.0%)	28,500±7790	(14.8±4.0%)	193,000±41,300†	(100±21.4%)

Results are expressed as the mean±SEM. N.D.; not detected. *$P<0.05$ vs any other group. †$P<0.01$ vs any other group.

1^+ cells (macrophages/granulocytes) and 13% of them were $CD3^+$ T cells which were almost all $TCR\alpha\beta^+$ and $CD4^+$. $CD161^+$ NK cells were hardly found in the non-cardiomyocytes (Table 3).

3.2. Staining of purified cell

Images of cells stained with May–Giemsa stain or naphthol AS-D chloroacetate esterase and α-naphthylbutyrate esterase stain in αβT cell and $CD11b^+$ cell fractions were compatible with typical images of T cells or macrophage/granulocytes. However, images of cells in a NCNI cell fraction differed from those of cardiomyocytes, T cells or macrophage/granulocytes. Cells in a NCNI cell fraction showed positive staining for α smooth muscle actin, Factor VIII related antigen or collagen III (Fig. 3).

3.3. Gene expression of immunological molecule in separated cells from EAM hearts

Gene expression of α-cardiac myosin, which should be found only in cardiomyocytes, was in fact detected only in a cardiomyocyte fraction and not in the other fractions (Table 4). T cell specific marker CD3 was detected in a αβT cell fraction but CD3 gene expression in the other fractions was under 5% presumably due to αβT cells contaminating those fractions and a few γδT cells in a NCNI cell fraction. CD11b, which should be found in macrophages and granulocytes, was expressed in a $CD11b^+$ cell fraction, but its gene expression in a αβT cell fraction was under 8% and that in the other fractions was under 3%, again presumed to be due to contaminating $CD11b^+$ cells. The fibroblast-specific marker (collagen type III) was detected in a NCNI cell fraction but its expression in the other fractions was under 1%. The endothelial cell-specific marker (von Willebrand factor) was detected in a NCNI cell fraction but its expression in the other fractions was under 10%. Because gene expression in smooth muscle cells is similar to that in cardiomyocytes and macrophages, it is difficult to find a specific marker for smooth muscle cells. However, generally speaking, because calponin [11] and caldesmo [12], which smooth muscle cells contain, were detected in a NCNI cell franction, most smooth muscle cells were presumed to be in that fraction.

Gene expression of cardiac myosin isoform and ANP was examined in purified cardiomyocytes after collagenase preparation and native cardiomyocytes, namely whole hearts immediately homogenated in Trizol, on days 0, 14, 21 and 28 to confirm that gene expression in cardiomyocytes was not influenced by collagenase preparation. Their ratios of copy numbers at each day to copy numbers at day 0 were almost equivalent for purified cardiomyocytes and native cardiomyocytes (Fig. 4).

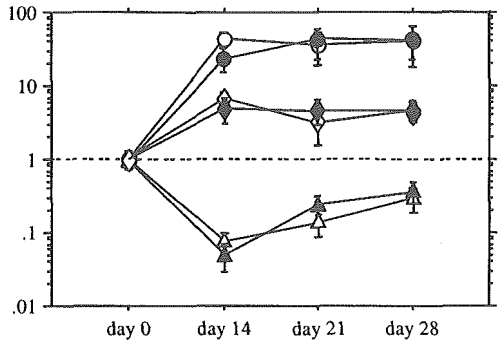

Fig. 4. mRNA copy numbers of α cardiac myosin, β cardiac myosin and ANP at each day/copy numbers at day 0. (>) ANP from purified cardiomyocytes. (⋆) ANP from whole heart. (△) α cardiac myosin from purified cardiomyocytes. (▲) α cardiac myosin from whole hearts. (◇) β cardiac myosin from purified cardiomyocytes. (◆) β cardiac myosin from whole hearts. Data obtained from quantitative RT-PCR were presented as mean±SEM.

Gene expression of immunological molecules was examined in fractions of purified cells (cardiomyocytes, $CD11b^+$ cells, αβT cells and NCNI cells) from day 18 EAM hearts (Table 5). Interleukin (IL)-2 and interferon (IFN)-γ were detected in a αβT cell fraction alone and IFN-γ receptor was detected in $CD11b^+$ cell, αβT cells, NCNI cell fractions and, to a lesser degree, in a cardiomyocyte fraction. IL-10 (Fig. 5A) and MCP-1 (Fig. 5B) in a NCNI cell fraction were significantly more than the other fractions and IL-10 receptor was detected in $CD11b^+$ cell and αβT cell fractions. TNF-α was detected in a $CD11b^+$ cell fraction and TNF-α receptor was detected in a NCNI cell fraction and, to a lesser degree, in $CD11b^+$ cell and cardiomyocyte fractions. Osteopontin was detected in $CD11b^+$ cell and NCNI cell fractions. One of its ligands, CD44, was found mainly in a αβT cell fraction, smaller amounts were found in $CD11b^+$ cell and NCNI cell fractions, and very little was found in a cardiomyocyte fraction. Most of programmed death-1 (PD-1) was detected in a αβT cell fraction and PD-1 ligand mainly in a $CD11b^+$ cell fraction. Fractalkine was detected in NCNI cell and cardiomyocyte fractions (Fig. 5C) and its receptor CX3CR1 in αβT cell and $CD11b^+$ cell fractions (Fig. 5D). Major histocompatibility complex (MHC) Class I and MHC Class II molecules were detected mostly in αβT cell and $CD11b^+$ cell fractions respectively, but both were detected in all fractions.

Expression of the genes for fractalkine, IFN-γ receptor, TNF-α receptor, CD44, MHC Class I and MHC Class II, thought to be present in cardiomyocytes, was examined in cardiomyocyte fractions of normal and day 18 and 90 EAM hearts (Table 6). Fractalkine, TNFα receptor, CD44, MHC Class I and MHC Class II expression significantly increased in a fraction of cardiomyocytes of acute myocarditis hearts.

Table 5
Absolute copy numbers of immunologic molecule mRNA in day 18 EAM hearts

	Copy numbers of mRNA/microgram of total RNA (copy numbers of mRNA)									
	Cardiomyocytes ($n=5$)		αβT cells ($n=5$)			$CD11b^+$ cells ($n=5$)			NCNI cells ($n=6$)	
IL-2	N.D.		329,000±103,000†	(100±31.3%)		N.D.			N.D.	
IFN-γ	N.D.		6,42,000±1,820,000†	(100±29.25%)		N.D.			N.D.	
INF-γ receptor	3,760,000±,944,000	(15.4±1.4%)	24,400,000± 4,070,000*	(100±16.7%)		15,800,000±2,870,000	(64.8±11.8%)		21,900,000±1,950,000	(89.8±8.0%)
IL-10	9,090±4,590	(0.34±17,)	240,000±96,200	(8.92±3.58%)		53,300±17,000	(1.98±0.63%)		2,690,000±951,000†	(100±35.4%)
IL-10 receptor	406,000±81,900	(5.29±1.07%)	6,050,000±2,170,000	(78.8±28.3%)		7,680,000±2,380,000	(100±.31.0%)		1,490,000±376,000	(19.4±4.90%)
TNF α	247,000±69,200	(1.35±0.38%)	2,560,000±699,000	(14.0±3.83%)		18,200,000±6,580,000†	(100±36.1%)		1,410,000±282,000	(7.73±1.55%)
TNF α receptor	4,440,000± 1,260,000	(11.7±3.33%)	2,380,000±448,000	(6.29±1.18%)		12,900,000±3,250,000	(34.1±8.59%)		37,800,000±4,860,000†	(100±11.2%)
MCP-1	754,000± 122,000	(0.70±0.11%)	1,870,000± 999,000	(1.73±0.93%)		7,590,000±2,510,000	(7.03±2.32%)		108,000,000±20,600,000†	(100±19.0%)
fractalkine	11,900,000±3,270	(56.1±15.4%)	236,000±107,000	(1.11±0.50%)		680,1000±346,000	(3.21±64%)		21,200,000±1,990,000†	(100±9.39%)
CX3CR1	812,000± 151,000	(10.4±1.93%)	7,810,000±1,950,000*	(100±25.0%)		3,920,000±1,098,000	(50.2±14.1%)		1,100,000,±262,000	(14.1±3.35%)
MCH Class I	41,700,000±2,480,000	(20.1±2.00%)	207,000,000±83,200,000*	(100±40.2%)		39,700,000±1,098,000	(19.2±5.76%)		63,700,000±8,920,000	(30.8±4.32%)
MHC Class II	319,000±5,300	(17.3±2.50%)	645,000±11,000	(35.6±11.5%)		1,840,000±535,000†	(100±29.1%)		358,000±70,700	(19.5±3.84%)
PD-1	8,380±5,300	(.13±0.055%)	16,500,00,± 180,000†	(100±31.4%)		26,300±17,300	(0.39±0.16%)		30,300±14,200	(0.18±0.09%)
PD-1L	198,000±80,300	(1.21±.49%)	5,360,000±1,570,000	(32.9±9.62%)		16,300,000±3,470,000†	(100±21.3%)		1,580,000±304,000	(9.69±1.86%)
osteopontin	3,140,000±791,000	(7.87±1.98%)	2,860,000±1,240,000,	(7.17±3.11%)		39,900,000±21,100,000	(100±54.3%)		24,400,000±4,360,000	(61.2±10.9%)
CD44	11,300,000±143,000	(8.7±1.11%)	129,000,000,±36,600,000*	(100±26.8%)		53,700,000±5,870,000	(41.5±4.54%)		48,300,000±14,300,000	(37.4±11.1%)

Results are expressed as the mean±SEM. N.D.; not detected. *$P<0.05$ vs any other group. †$P<0.01$ vs any other group.

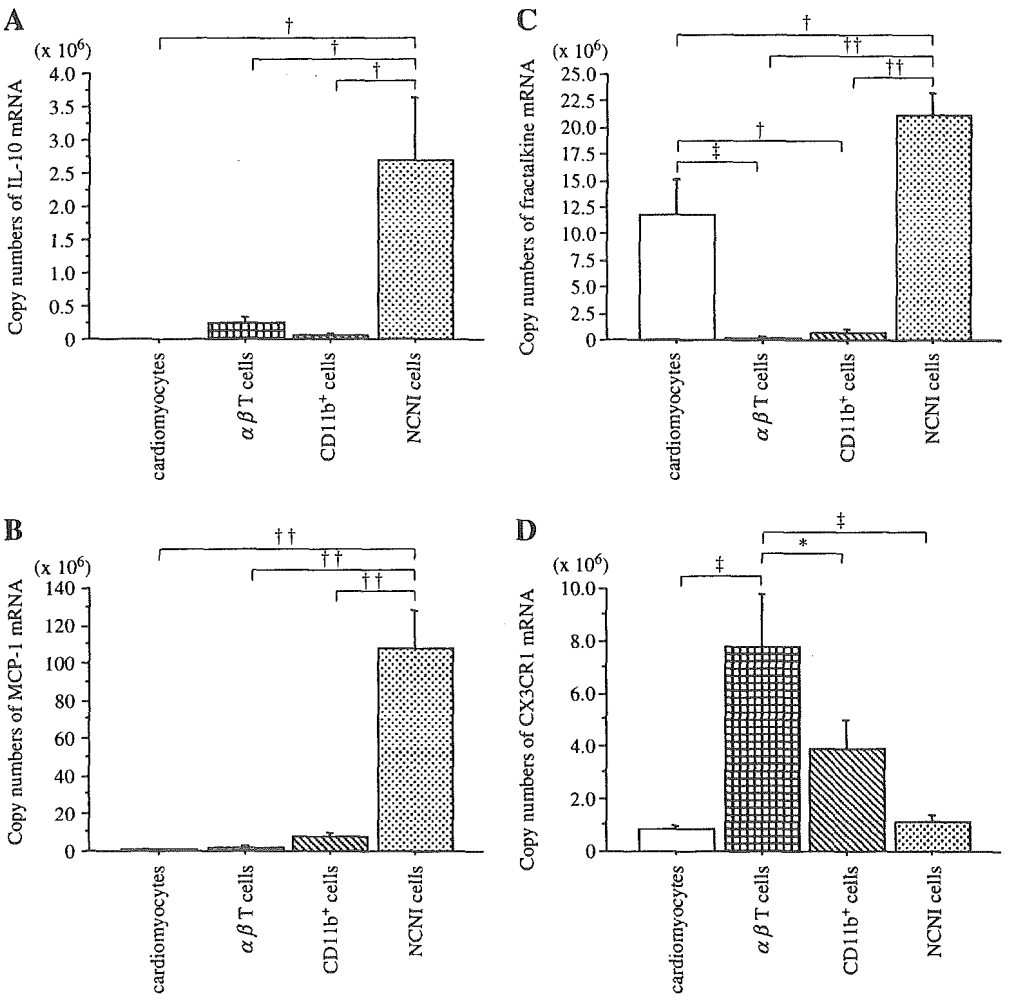

Fig. 5. Absolute copy numbers of immunological molecule mRNA/microgram of total RNA in day 18 EAM hearts. Data obtained from quantitative RT-PCR were presented as mean±SEM. (A) IL-10. (B) MCP-1. (C) Fractalkine. (D) CX3CR1. *$P<0.05$, †$P<0.01$, ‡$P<0.001$, and ††$P<0.0001$.

3.4. Effect of TNF-α on gene expression of immunological molecules in cultivated NC cells from EAM hearts

Because NCNI cells strongly expressed TNF-α receptor (Table 2), we examined the effect of TNF-α on fractalkine, MCP-1 and osteopontin which they expressed. In cultivated NC cells containing fibroblasts, smooth muscle cells, endothelial cells and CD11b$^+$ cells, fractalkine (160 ng/ml of TNF-α group, 20.0±4.8-fold, $P<0.001$) and MCP-1 (160 ng/ml of TNF-α group, 63.2±8.0-fold, $P<0.0001$) were significantly upregulated by TNF-α (Fig. 6A and B). However, we could not find the significant influence of gene expression of osteopontin by TNF-α in cultivated NC cells (Fig. 6C).

Table 6
Absolute copy numbers of mRNA in cardiomyocytes of EAM hearts

	Copy numbers of mRNA/microgram of total RNA		
	Normal ($n=5$)	Day 18 ($n=5$)	Day 90 ($n=6$)
Fractalkine	4,880,000±998,000	11,900,000±3,270,000*	4,420,000±667,000
INF-γ recptor	4,440,000±639,000	3,760,000±944,000	2,690,000±382,000
TNF-α receptor	576,000±90,100	5,130,000±1,610,000†	703,000±204,000
CD44	1,060,000±140,000	11,300,000±1,430,000†	2,540,000±149,000
MHC Class I	3,150,000±901,000	41,700,000±480,000†	5,450,000±1,150,000
MHC Class II	N.D.	319,000±46,000†	7160±2870

Results are expressed as the mean±SEM. N.D.; not detected. *$P<0.05$ vs any other group. †$P<0.01$ vs any other group.

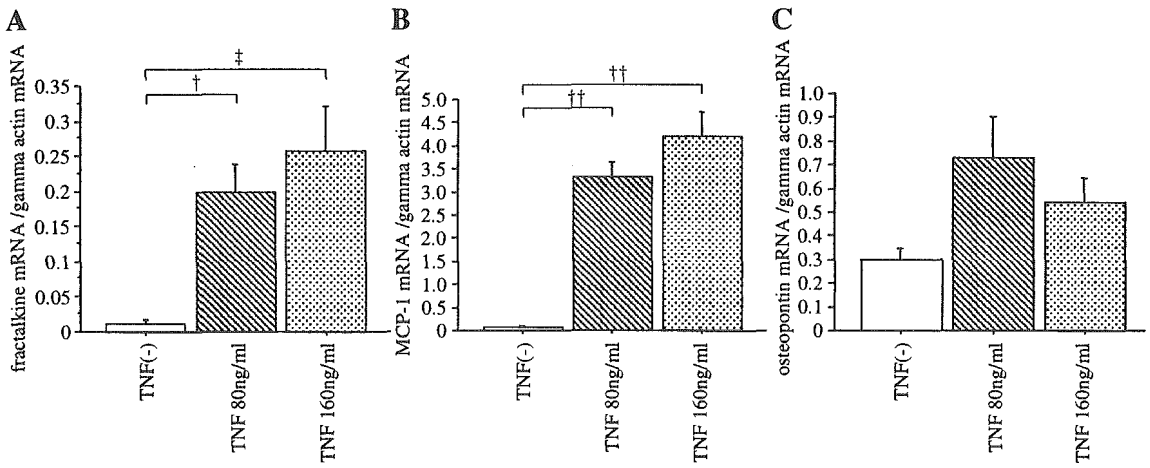

Fig. 6. Copy numbers of immunological molecule mRNA/copy numbers of γ-actin mRNA in cultivated NC cells from EAM hearts with TNF-α. Data obtained from quantitative RT-PCR were presented as mean ± SEM. (A) Fractalkine. (B) MCP-1. (C) Osteopontin. Fractalkine and MCP-1 were significantly increased by TNF-α. No significant increase of osteopontin by TNF-α was observed. $^{\dagger}P<0.01$, $^{\ddagger}P<0.001$, and $^{\dagger\dagger}P<0.0001$.

3.5. Immunostaining of osteopontin

Osteopontin expression was observed in some mononuclear cells infiltrating into EAM hearts on day 18 (Fig. 7B). However, osteopontin expression was hardly detected in normal heart (Fig. 7C).

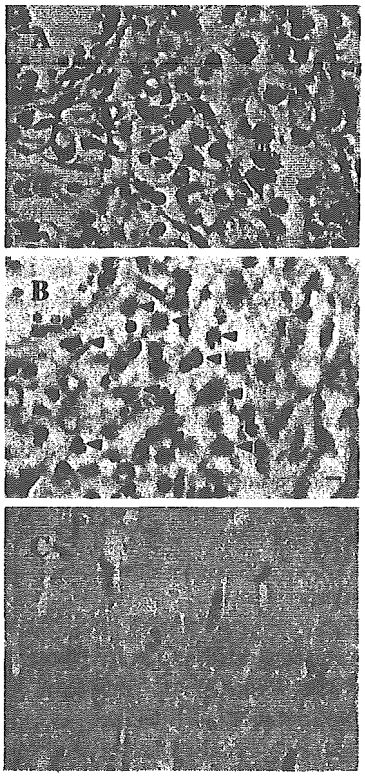

Fig. 7. (A) A section of EAM heart on day 18 was stained with hematoxylin and eosin stain. (B) The same section as A was stained with anti-osteopontin antibodies. The immunoreactivity was observed in some mononucleated cells. Arrowheads indicate positive staining. (C) A section of normal heart was stained with anti-osteopontin antibodies. The immunoreactivity was hardly observed. Bar represents 10 μm.

4. Discussion

In this study, gene expression of some immunological molecules (fractalkine, IL-10, MCP-1, CD44, IFN-γ receptor, TNFα receptor, etc.) was found in non-inflammatory cells. This suggests that they may be mediators not only for inflammatory cell activity but also for originally constitutive cells in the heart—cardiomyocyte and NCNI cells.

Fractalkine has been identified as a novel chemokine that exhibits cell adhesion and chemoattractive properties in the central nervous system [13]. It is interesting that fractalkine mRNA is found in purified cardiomyocytes and NCNI cells. This result supports previous reports that endothelial cells of the coronary vasculature and endocardium were the principal source of fractalkine and some fractalkine immunoreactivity was also found on the myocytes [14]. Normal cardiomyocytes express some fractalkine, but during the acute phase of inflammation expression increases. TNF-α produced by $CD11b^{+}$ cells in EAM hearts strongly upregulated fractalkine mRNA in cultivated NC cells. It has been reported that fractalkine expression is markedly induced by inflammatory cytokines, TNF-α, IL-1 and IFN-γ in primary cultured endothelial cells [15,16]. Because cytokines as TNF-α, IL-1β or IFN-γ increase in EAM hearts [5], fractalkine mRNA in cardiomyocytes of EAM hearts may be upregulated. CX3CR1, receptor of fractalkine, was found in $CD11b^{+}$ cells and αβT cells. This suggests that cytokines produced by inflammatory cells increase fractalkine on residential cells and then it attracts and activates inflammatory cells in EAM hearts. Recently, it was reported that fractalkine was secreted by central nervous system neurons and astrocytes [17]. Neuronal

fractalkine expression in virus encephalitis plays important roles in macrophage recruitment and neuroprotection in the central nervous system [18]. Fractalkine may play a similar role in the heart.

IL-10 was expressed unexpectedly in NCNI cells. Before this study, we thought that cells expressing IL-10 were Th2 cytokine-secreting T cells. We could detect IL-2 and IFN-γ gene expression in αβT cells, but IL-10 gene expression was barely detected in them. Gene expressions of IL-4 and IL-13 (Th2 cytokines), which are produced only by hemopoietic cells, were not found in EAM whole hearts on days 18 and 28 by using quantitative RT-PCR [data not shown]. Therefore, it is thought that αβT cells in acute EAM hearts secrete Th1 but not Th2 cytokine. Previously, we reported that IL-10 producing cells in peripheral blood increased on day 28 in EAM, however, on day 28, most parts of the infiltrating cells disappeared and the fibrosis remained in the myocardium [19]. In rheumatoid arthritis, IL-10 is released by fibroblast-like synoviocytes [20]. It may be that, in EAM hearts, fibroblasts, not T cells, secrete most of IL-10 and it modulate $CD11b^+$ and αβT cells expressing IL-10 receptors by paracrine mechanisms. It has been reported that IL-10 gene therapy ameliorated EAM and other models of autoimmune inflammatory disease [21], therefore NCNI cells producing IL-10 may play an important role for EAM.

It has been reported that MCP-1 is secreted by activated lymphocytes, macrophages, endothelial cells, smooth muscle cells and platelet-derived growth factor-activated fibroblasts [22–24]. Our previous immunohistochemistry analysis in EAM showed that large monocytes were stained by anti-MCP-1 antibody [25]. This study suggests that they are not macrophages but NCNI cells, which attract macrophages into myocarditis hearts by paracrine mechanisms. It has been reported that MCP-1 secretion was regulated by the proinflammatory cytokines, IL-1 and TNF-α in colonic subepithelial myofibroblasts [26]. In this study, we also showed that MCP-1 mRNA in cultivated NC cells from EAM hearts were upregulated by TNF-α. Increase of TNF-α and IL-1β produced by macrophages in EAM hearts [5] upregulates expression of MCP-1 gene in NCNI cells and it may attract macrophage.

We previously reported that large amounts of osteopontin mRNA are expressed in early EAM [5]. Osteopontin protein was detected in EAM hearts by immunohistochemistry. Osteopontin is an extracellular matrix protein as well as a cytokine that contributes to the development of Th1 immunity [27]. Osteopontin is secreted by $CD11b^+$ cells and NCNI cells. It may activate T cells expressing CD44 as one of the ligands for osteopontin [28]. It may also modulate $CD11b^+$ cells, NCNI cells and to a lesser degree probably cardiomyocytes in myocarditis. Osteopontin is also a potentially important mediator of AII regulation of cardiac fibroblast behavior in the cardiac remodeling process [29].

PD-1 deficiency causes a variety of autoimmune diseases [30] and dilated cardiomyopathy with severely impaired contraction and death by congestive heart failure [31]. It has been reported that the parenchymal cells of heart, lung and kidney constitutively express PD-1 ligand [30]. Cytokine such as IFN-γ or other inflammatory stimuli induces PD-1 ligand expression [32]. In this study, $CD11b^+$ cells in EAM hearts expressed both IFN-γ receptor and PD-1 ligand. $CD11b^+$ cells stimulated by IFN-γ may regulate αβT cells activation in EAM by PD-1–PD1 ligand binding. However, more evidence is needed to support this concept.

$CD4^+$T cells play important roles in EAM. MHC Class II expressing cells that can bind CD4 are mainly $CD11b^+$ cells. Some papers reported that MHC Class I and MHC Class II expression increases in myocarditis hearts or DCM [33–35]. This suggest that their expression in cardiomyocytes in acute myocarditis increased, which may mean that lymphocytes have contact with cardiomyocytes in acute myocarditis more closely than in normal heart or in chronic myocarditis.

This method of isolating and purifying the subgroups of cells from myocarditis hearts by using stainless-steel sieves at 4 °C is thought not to damage cells in contrast to purification by centrifuge in Percoll [36]. Actually, the gene expression of cardiac myosin isoform and ANP [5], which is found only in cardiomyocytes, was the same in purified cardiomyocytes as in unpurifed whole hearts. Therefore we assume that the gene expression in purified cell fractions is practically unchanged by these preparations.

It was reported that immunological factors might be of greater prognostic importance than the more conventional assessments of the hemodynamic and clinical status [7]. It is clinically significant to define the mechanisms by which these factors influence cardiac function and remodeling. Our study indicated that inflammatory cells and non-inflammatory cells influenced each other. It is to be hoped that a clarification of the mechanism lead to therapies for myocarditis and DCM by regulation of immunological factors.

We present here a possible crosstalk by immunological molecules among constitutive cells in EAM hearts. They play important roles not only among inflammatory cells but also among non-inflammatory cells containing cardiomyocytes, fibroblasts, endothelial cells and smooth muscle cells.

Acknowledgments

This study was supported in part by grants for scientific research from the Ministry of Education, Science and Culture of Japan (number 14570645).

References

[1] Kodama M, Matsumoto Y, Fujiwara M, Masani F, Izumi T, Shibata A. A novel experimental model of giant cell myocarditis induced in rats by immunization with cardiac myosin fraction. Clin Immunol Immunopathol 1990;57:250–62.

[2] Kodama M, Hanawa H, Saeki M, Hosono H, Inomata T, Suzuki K, et al. Rat dilated cardiomyopathy after autoimmune giant cell myocarditis. Circ Res 1994;75:278–84.
[3] Hanawa H, Tsuchida M, Matsumoto Y, Watanabe H, Abo T, Sekikawa H, et al. Characterization of T cells infiltrating the heart in rats with experimental autoimmune myocarditis. Their similarity to extrathymic T cells in mice and the site of proliferation. J Immunol 1993;150: 5682–95.
[4] Kodama M, Zhang S, Hanawa H, Shibita A. Immunohistochemical characterization of infiltrating mononuclear cells in the rat heart with experimental autoimmune giant cell myocarditis. Clin Exp Immunol 1992;90:330–5.
[5] Hanawa H, Abe S, Hayashi M, Yoshida T, Yoshida K, Shiono T, et al. Time course of gene expression in rat experimental autoimmune myocarditis. Clin Sci 2002;103:623–32.
[6] Okura Y, Yamamoto T, Goto S, Inomata T, Hirono S, Hanawa H, et al. Characterization of cytokine and iNOS mRNA expression in situ during the course of experimental autoimmune myocarditis in rats. J Mol Cell Cardiol 1997;29:491–592.
[7] Rauchhaus M, Doehner W, Francis DP, Davos C, Kemp M, Liebenthal C, et al. Plasma cytokine parameters and mortality in patients with chronic heart failure. Circulation 2000;102:3060–7.
[8] Hwang TC, Horie M, Nairn AC, Gadsby DC. Role of GTP-binding proteins in the regulation of mammalian cardiac chloride conductance. J Gen Physiol 1992;99:465–89.
[9] Isenberg G, Klockner U. Calcium tolerant ventricular myocytes prepared by preincubation in a "KB medium". Pflugers Arch 1982;395:6–18.
[10] Toba K, Hanawa H, Fuse I, Sakaue M, Watanabe K, Uesugi Y, et al. Difference in CD22 molecules in human B cells and basophils. Exp Hematol 2002;30:205–11.
[11] Ya J, Markman MW, Wagenaar GT, Blommaart PJ, Moorman AF, Lamers WH. Expression of the smooth-muscle proteins alpha-smooth-muscle actin and calponin, and of the intermediate filament protein desmin are parameters of cardiomyocyte maturation in the prenatal rat heart. Anat Rec 1997;249:495–505.
[12] Hayashi K, Yano H, Hashida T, Takeuchi R, Takeda O, Asada K, et al. Genomic structure of the human caldesmon gene. Proc Natl Acad Sci U S A 1992;89:12122–6.
[13] Bazan JF, Bacon KB, Hardiman G, Wang W, Soo K, Rossi D, et al. A new class of membrane-bound chemokine with a CX3C motif. Nature 1997;385:640–4.
[14] Harrison JK, Jiang Y, Wees EA, Salafranca MN, Liang HX, Feng L, et al. Inflammatory agents regulate in vivo expression of fractalkine in endothelial cells of the rat heart. J Leukoc Biol 1999;66:937–44.
[15] Fraticelli P, Sironi M, Bianchi G, D'Ambrosio D, Albanesi C, Stoppacciaro A, et al. Fractalkine (CX3CL1) as an amplification circuit of polarized Th1 responses. J Clin Invest 2001;107:1173–81.
[16] Garcia GE, Xia Y, Chen S, Wang Y, Ye RD, Harrison JK, et al. NF-kappaB-dependent fractalkine induction in rat aortic endothelial cells stimulated by IL-1beta, TNF-alpha, and LPS. J Leukoc Biol 2000; 67:577–84.
[17] Hatori K, Nagai A, Heisel R, Ryu JK, Kim SU. Fractalkine and fractalkine receptors in human neurons and glial cells. J Neurosci Res 2002;69:418–26.
[18] Tong N, Perry SW, Zhang Q, James HJ, Guo H, Brooks A, et al. Neuronal fractalkine expression in HIV-1 encephalitis: roles for macrophage recruitment and neuroprotection in the central nervous system. J Immunol 2000;164:1333–9.
[19] Fuse K, Kodama M, Ito M, Okura Y, Kato K, Hanawa H, et al. Polarity of helper T cell subsets represents disease nature and clinical course of experimental autoimmune myocarditis in rats. Clin Exp Immunol 2000;134:403–8.
[20] Ritchlin C, Haas-Smith SA. Expression of interleukin 10 mRNA and protein by synovial fibroblastoid cells. J Rheumatol 2001; 28:698–705.
[21] Watanabe K, Nakazawa M, Fuse K, Hanawa H, Kodama M, Aizawa Y, et al. Protection against autoimmune myocarditis by gene transfer of interleukin-10 by electroporation. Circulation 2001; 104:1098–100.
[22] Antoniades HN, Neville-Golden J, Galanopoulos T, Kradin RL, Valente AJ, Graves DT. Expression of monocyte chemoattractant protein 1 mRNA in human idiopathic pulmonary fibrosis. Proc Natl Acad Sci U S A 1992;89:5371–5.
[23] Ozaki K, Hanazawa S, Takeshita A, Chen Y, Watanabe A, Nishida K, et al. Interleukin-1 beta and tumor necrosis factor-alpha stimulate synergistically the expression of monocyte chemoattractant protein-1 in fibroblastic cells derived from human periodontal ligament. Oral Microbiol Immunol 1996;11:109–14.
[24] Yoshimura T, Leonard EJ. Secretion by human fibroblasts of monocyte chemoattractant protein-1, the product of gene JE. J Immunol 1990;144:2377–83.
[25] Fuse K, Kodama M, Hanawa H, Okura Y, Ito M, Shiono T, et al. Enhanced expression and production of monocyte chemoattractant protein-1 in myocarditis. Clin Exp Immunol 2001;124:346–52.
[26] Okuno T, Andoh A, Bamba S, Araki Y, Fujiyama Y, Fujiyama M, et al. Interleukin-1beta and tumor necrosis factor-alpha induce chemokine and matrix metalloproteinase gene expression in human colonic subepithelial myofibroblasts. Scand J Gastroenterol 2002;37:317–24.
[27] Ashkar S, Weber GF, Panoutsakopoulou V, Sanchirico ME, Jansson M, Zawaideh S, et al. Eta-1 (osteopontin): an early component of type-1 (cell-mediated) immunity. Science 2000;287:860–4.
[28] Weber GF, Ashkar S, Glimcher MJ, Cantor H. Receptor-ligand interaction between CD44 and osteopontin (Eta-1). Science 1996; 271:509–12.
[29] Ashizawa N, Graf K, Do YS, Nunohiro T, Giachelli CM, Meehan WP, et al. Osteopontin is produced by rat cardiac fibroblasts and mediates A(II)-induced DNA synthesis and collagen gel contraction. J Clin Invest 1996;98:2218–27.
[30] Nishimura H, Honjo T. PD-1: an inhibitory immunoreceptor involved in peripheral tolerance. Trends Immunol 2001;22:265–8.
[31] Nishimura H, Okazaki T, Tanaka Y, Nakatani K, Hara M, Matsumori A, et al. Autoimmune dilated cardiomyopathy in PD-1 receptor-deficient mice. Science 2001;291:319–22.
[32] Freeman GJ, Long AJ, Iwai Y, Bourque K, Chernova T, Nishimura H, et al. Engagement of the PD-1 immunoinhibitory receptor by a novel B7 family member leads to negative regulation of lymphocyte activation. J Exp Med 2000;192:1027–34.
[33] Herskowitz A, Ahmed-Ansari A, Neumann DA, Beschorner WE, Rose NR, Soule LM. Induction of major histocompatibility complex antigens within the myocardium of patients with active myocarditis: a nonhistologic marker of myocarditis. J Am Coll Cardiol 1990;15: 624–32.
[34] Noutsias M, Seeberg B, Schultheiss HP, Kuhl U. Expression of cell adhesion molecules in dilated cardiomyopathy: evidence for endothelial activation in inflammatory cardiomyopathy. Circulation 1999;99: 2124–31.
[35] Wojnicz R, Nowalany-Kozielska E, Wojciechowska C, Glanowska G, Wilczewski P, Niklewski T, et al. Randomized, placebo-controlled study for immunosuppressive treatment of inflammatory dilated cardiomyopathy: two-year follow-up results. Circulation 2001;104: 39–45.
[36] Harada M, Saito Y, Kuwahara K, Ogawa E, Ishikawa M, Nakagawa O, et al. Interaction of myocytes and nonmyocytes is necessary for mechanical stretch to induce ANP/BNP production in cardiocyte culture. J Cardiovasc Pharmacol 1998;31:S357–9.

Molecular and Cellular Biochemistry 269: 137–142, 2005.

Effects of angiotensin-II receptor blocker candesartan cilexetil in rats with dilated cardiomyopathy

Ken Shirai,[1] Kenichi Watanabe,[1] Meilei Ma,[1] Mir I I Wahed,[1] Mikio Inoue,[1] Yuki Saito,[1] Palaniyandi Selvaraj Suresh,[1] Takeshi Kashimura,[2] Hitoshi Tachikawa,[2] Makoto Kodama[2] and Yoshifusa Aizawa[2]

[1]*Department of Clinical Pharmacology, Niigata University of Pharmacy and Applied Life Sciences, Niigata City, Japan;*
[2]*First Department of Medicine, Niigata University School of Medicine, Niigata City, Japan*

Received 19 March 2004; accepted 27 August 2004

Abstract

We examined effects of an angiotensin-II receptor blockers, candesartan cilexetil, in rats with dilated cardiomyopathy after autoimmune myocarditis. Candesartan cilexetil showed angiotensin-II blocking action in a dose-dependent manner in rats with dilated cardiomyopathy. Twenty-eight days after immunization, surviving Lewis rats were divided into four groups and given candesartan cilexetil at 0.05 mg/kg, 0.5 mg/kg or 5 mg/kg per day (Group-C0.05, $n = 15$, Group-C0.5, $n = 15$ and Group-C5, $n = 15$, respectively) or vehicle alone (Group-V, $n = 15$). After oral administration for 1 month, the left ventricular end-diastolic pressure and heart weight/body weight ratio were lower in Group-C0.05 (13.3 ± 1.1 mmHg and 3.7 ± 0.2 g/kg, respectively), in Group-C0.5 (8.0 ± 0.9 mmHg and 3.3 ± 0.1 g/kg, respectively) and in Group-C5 (5.5 ± 1 mmHg and 3.1 ± 0.1 g/kg, respectively) than in Group-V (13.5 ± 1.0 mmHg and 3.8 ± 0.2 g/kg, respectively). The area of myocardial fibrosis was also lower in Group-C0.05 (25 ± 3%), in Group-C0.5 (20 ± 3%), and in Group-C5 (12 ± 1%) than in Group-V (32±4%). Furthermore, expressions of transforming growth factor-β1 and collagen-III mRNA were suppressed in Group-C0.05 (349±23% and 395±22%, respectively), Group-C0.5 (292±81% and 364±42%, respectively) and in Group-C5 (204±63% and 259±33%, respectively) compared with those in Group-V (367±26% and 437±18%, respectively). These results suggest that candesartan cilexetil can improve the function of inefficient heart. (Mol Cell Biochem 269: 137–142, 2005)

Key words: angiotensin receptor blockade, heart failure, candesartan, angiotensin-II, dilated cardiomyopathy, transforming growth factor-β1, collagen-III

Introduction

At present, various medicines are being used to treat heart failure, particularly for β-blockers and angiotensin-converting enzyme inhibitors (ACEI), it has been demonstrated that these medicines improved the prognosis of heart failure in various large-scale clinical trials [1–3]. However, recent evidence suggests that production of angiotensin (Ang)-II involves not only ACE but also chymase, and Ang-II produced in local tissue participates in organ injury. Angiotensin-II

Address for offprints: K. Watanabe, Department of Clinical Pharmacology, Niigata University of Pharmacy and Applied Life Sciences, Kamishinei-Cho 5-13-2, Niigata City 950-2081, Japan (E-mail: watanabe@niigata-pharm.ac.jp)

receptor blockers (ARB) and ACEI have been shown to reduce mortality and morbidity in patients and an animal model with heart failure [1–5].

The transition from compensated to failing cardiac hypertrophy has been attenuated to a reversal to a fetal pattern of cardiomyocyte gene expression and to adverse remodeling of the ventricular connective tissue matrix [6, 7]. Many kinds of growth factor, Ang-II, transforming growth factor (TGF)-β1 and collagen-III, have been suggested to play important roles in structural remodeling of the non-myocyte compartment of the myocardium following heart failure [8, 9]. It is therefore important to determine whether ARB has any effect on fetal gene expression or extracellular matrix remodeling in methods not only with heart failure after myocardial infarction, but also with dilated cardiomyopathy.

Recently, the utility of candesartan in chronic heart failure (CHF) has been demonstrated in CHARM (Candesartan in Heart failure: Assessment of Reduction in Mortality and morbidity) trial [10]. It is worth noting that this trial demonstrated that candesartan is the first ARB to improve the survival rate in patients with CHF complicating left-ventricular depression, regardless of whether ARB administration was combined with ACEI [11].

In the present study, the inhibitory action against Ang-II and the cardioprotective properties of ARB candesartan cilexetil (candesartan) were studied in a rat model of dilated cardiomyopathy. The effects of long-term treatment with ARB on the development of myocardial damage were then examined. We found that candesartan can block blood pressure increases caused by circulating Ang-II and provide sufficient protection against injury by the renin-angiotensin system in rats with dilated cardiomyopathy.

Materials and methods

Animals

Nine-week-old male Lewis rats were obtained from Charles River Japan Inc. (Kanagawa, Japan). The morbidity of experimental autoimmune myocarditis was 100% in rats immunized using our protocol [12–14]. Age-matched normal control group (Group-N) consisted of eight normal Lewis rats.

Assessment of the inhibitory actions of candesartan on angiotensin-II-induced blood pressure increases in rats with heart failure

Six weeks after immunization, surviving rats were used for this experiment. Rats were anesthetized with pentobarbital sodium (50 mg/kg, intraperitoneally; each group, $n = 5$). Under aseptic conditions, a catheter prepared by connecting polyethylene tubing (PE 10 and PE 50; Becton Dickson and Co., Parsippany, NJ, USA) filled with sterile heparin sodium (200 U/ml) was inserted into the abdominal aorta via the femoral artery, guided under the skin and exteriorized at the back of the neck. A catheter filled with heparin was inserted into the external jugular vein, guided under the skin of the neck and exteriorized at the back of the neck. Each rat was injected subcutaneously with penicillin G (2000 U) and streptomycin (20 mg) to prevent infection. After 4–5 days, the rats were placed in cages and acclimatized to the measurement of blood pressure and injection of Ang-I while conscious. Before administration of drugs, Ang-I was infused in a stepwise manner (each dose was infused for 2 min) through the venous catheter from 0.1 to 3 μg/kg per min to obtain the dose-response curve as a control. Rats were then treated orally with a single bolus by gastric gavage with candesartan or vehicle (0.5% methylcellulose). Four hours after drug administration, when the drugs exhibited the maximal hypotensive effects, Ang-I was infused in the same manner from 0.3 to 10 μg/kg per min (candesartan 0.1 mg/kg) or 1 to 30 μg/kg per min (candesartan 0.5, 5 and 10 mg/kg). Animals were used repeatedly after a recovery period of 2 or more days. The blood pressure was measured using a pressure transducer (P 10 EX-1; NEC Medical Systems, Tokyo, Japan) and recorded with a bridge amplifier on a Power Lab system (Power Lab/8 sp: AD Instruments, Castle Hill, Australia).

Medication

Twenty-eight days after immunization, the surviving rats were divided into four groups for oral administration for 1 month: Group-C0.05, 0.05 mg/kg candesartan per day (low-dose group, $n = 15$); Group-C0.5, 0.5 mg/kg candesartan per day (middle-dose group, $n = 15$); Group-C5, 5mg/kg candesartan per day (high-dose group, $n = 15$); or Group-V, vehicle alone (0.5% methylcellulose, $n = 15$).

Throughout the studies, all animals were treated in accordance with the guidelines for animal experimentation at our institute [14].

Hemodynamic study

Rats were anesthetized with 2% halothane in O_2 during the surgical procedures to measure the hemodynamic parameters, and then this concentration was reduced to 0.5% to minimize the hemodynamic affects. The central venous pressure (CVP), mean arterial blood pressure (mean BP), peak left ventricular pressure (LVP), left ventricular end-diastolic pressure (LVEDP), and rates of intraventricular pressure rise and decline ($\pm$dP/dt) were recorded as described previously [14].

Histopathology

After measurement of hemodynamic parameters, the heart was immediately removed and weighted, then the ratio of heart weight/body weight (g/kg) was calculated. The heart specimens were cut into 2-mm transverse slices and fixed in 10% formalin for histological examination. The preparations were stained with Azan-Mallory. Using these specimens, the area of myocardial fibrosis was quantified using a color image analyzer (CIA-102; Olympus, Tokyo, Japan), using the differences in color (blue fibrotic area as opposed to red myocardium). The results were presented as the ratio of the fibrotic area to the area of myocardium [14].

Ribonuclease protection assay

Apical left ventricles from all groups were rapidly excised, frozen in acetone ice, and stored at −80 °C. Antisense complementary RNA probes for TGF-β1, collagen-III and glyceraldehydes-3-phosphate dehydrogenase (GAPDH) were generated as described previously [15–17]. The ribonuclease protection assays for quantification of TGF-β1 and collagen-III mRNA levels were performed as described previously [15–17]. The results for each mRNA were normalized to those for GAPDH mRNA in each sample.

Statistical analysis

Data are presented as the mean ± S.E.M.. Statistical assessment of the groups was performed by one-way analysis of variance, followed by Tukey's method.

Results

The inhibitory actions of candesartan on angiotensin-II-induced increases in blood pressure in rats with heart failure

Injection of Ang-I evoked hypertension in all groups. The maximal increase in mean BP from the baseline value during Ang-I injection was about 40 mmHg in all groups (Fig. 1). Treatment with candesartan inhibited these responses in a dose-dependent manner.

Clinical course

Four of 15 rats (27%) in Groups-V and -C0.05, 2 of 15 rats (13%) in Group-C0.5, and 1 of 15 rats (7%) in Group-C5 died between days 30 and 56. All hearts from these rats showed extensive myocardial fibrosis and massive pericardial effusion. None of the animals in Group-N died (Table 1).

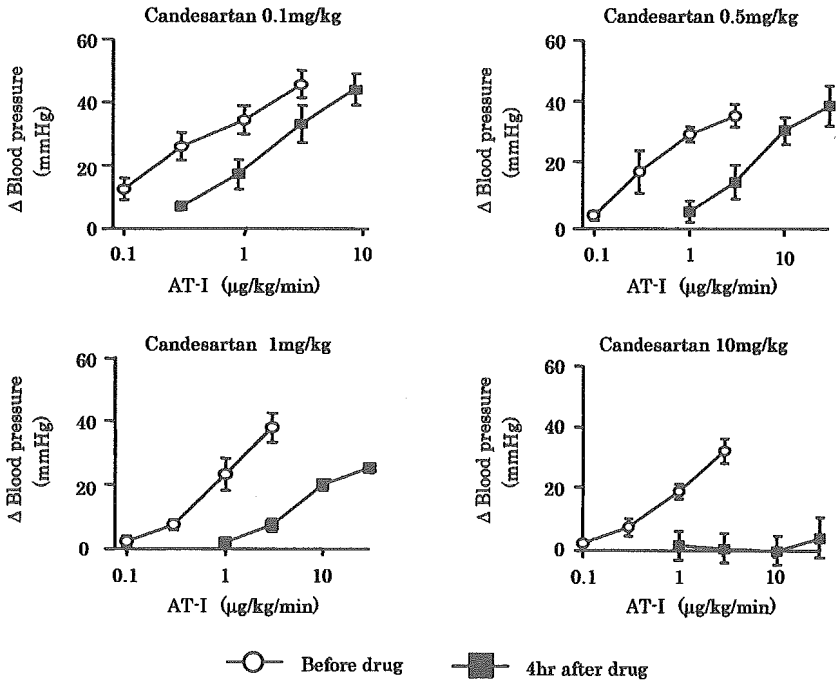

Fig. 1. The inhibitory effects of candesartan on angiotensin (AT)-II-induced increases in blood pressure in rats with dilated cardiomyopathy. Treatment with candesartan inhibited these responses in a dose-dependent manner. Δblood pressure, increase in mean blood pressure after AT-I administration; AT-I, angiotensin-I.